ACS OMEGA

Open Access

http://pubs.acs.org/journal/acsodf

Article

Geochemical Evaluation of Paleocene Source Rocks in the Kohat Sub-Basin, Pakistan

Jazeb Sohail,[#] Saqib Mehmood, Samina Jahandad, Muhsan Ehsan,[*,#] Kamal Abdelrahman, Abid Ali,[*] S. M. Talha Qadri, and Mohammed S. Fnais

Cite This: *ACS Omega* 2024, 9, 14123−14141

Read Online

ACCESS | Metrics & More | Article Recommendations

ABSTRACT: The Kohat sub-basin is one of the main hydrocarbon-producing sedimentary basins located in the northwest extension of the Indus Basin in Pakistan. It contains numerous proven and potential petroleum from the Cambrian to the Miocene. Conventional petroleum resources have been depleting rapidly over the last couple of years. Therefore, unconventional resources should be explored using a variety of geochemical and geophysical techniques to address the energy demands. Geochemical techniques, including total organic carbon (TOC) assessment, Rock-Eval pyrolysis, organic petrography, and biomarker studies, are essential for evaluating the potential of shale gas reservoirs to delineate future prospects in a basin. The source rock potential of the Paleocene rocks, including the Patala, Lockhart, and Hangu formations of the sub-basin, is evaluated using geochemical analyses on well cuttings from the Tolanj-01 well. The analyses include estimation of total organic carbon (TOC), Rock-Eval pyrolysis, and organic petrography (vitrinite reflectance) to evaluate the organic richness, thermal maturity, kerogen type, hydrocarbon type, and environment of deposition. Other techniques for extractable organic matter (EOM) include solid−liquid chromatographic separation of fractions, gas chromatography (GC-FID)/whole oil chromatography, and gas chromatography−mass spectrometry (GC-MS). The organic matter (TOC, wt %) analysis reveals that 18 (18) samples of the Hangu formation (0.08−1.8 wt %) show poor values, 12 (12) samples of the Lockhart formation (0.05−0.5 wt %) have poor to fair content, and 26 (26) samples of the Patala formation have poor to fair (0.08−0.19 wt %) TOC content. Rock-Eval pyrolysis studies including hydrogen index, oxygen index, T_{max}, quantities of free hydrocarbons (S_1, mg/g), and hydrocarbons produced from pyrolysis (S_2, mg/g) are determined for the well-cut samples (56) of the Paleocene rocks. The hydrogen index values for the Hangu formation are lower than 200, and those for the Lockhart and Patala formations range between 100 and 250. A maceral analysis is also conducted on these samples, which reveal that the majority of the samples of the Paleocene units present in the basin belong to kerogen types II/III. The thermal maturity of the Hangu and Lockhart formations falls in the late-stage oil window, while that of the Patala formation falls in the peak to late oil window. The genetic potential (GP) for these rock units is also determined based on S_1 and S_2 values, which reveals that it is generally poor except for a few samples of the Hangu and Lockhart formations, which show fair GP values. For the organic petrography (vitrinite reflectance, R_0), one sample from each unit is selected, which shows that the Hangu, Lockhart, and Patala formations fall in the category of the mature oil window with their R_0 (%) values being 0.95, 0.89, and 0.82, respectively. The extracts (EOM) from these rock units are also analyzed to assess the depositional settings, biological source input, biodegradation, thermal maturity, etc. The greater values of pristine to phytane (Pr/Ph > 1) ratios for Hangu (1.33), Lockhart (1.23), and Patala (1.8) indicate an intermediate condition (suboxic), while a cross-plot of Pr/n-C_{17}−Ph/n-C_{18} shows that the organic matter is deposited in a transitional setting. The ratios between C_{19}TCT/C_{19} TCT + C_{23} TCT and C_{24} TeCT/C_{24}TeCT + C_{23}TCT biological source inputs are mainly of marine origin. Similarly, the ternary diagram of regular steranes (C_{27}−C_{28}−C_{29}) shows a greater marine input. Lower values of the carbon preference index (CPI1) for Hangu (0.95), Lockhart (0.91), and Patala (1.04) indicate higher thermal maturity of the Paleocene rocks. Similarly, the

continued...

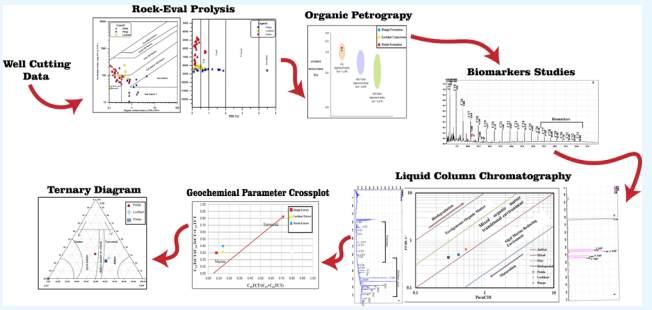

Received: December 2, 2023
Revised: February 21, 2024
Accepted: February 27, 2024
Published: March 15, 2024

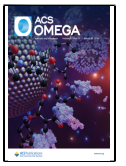

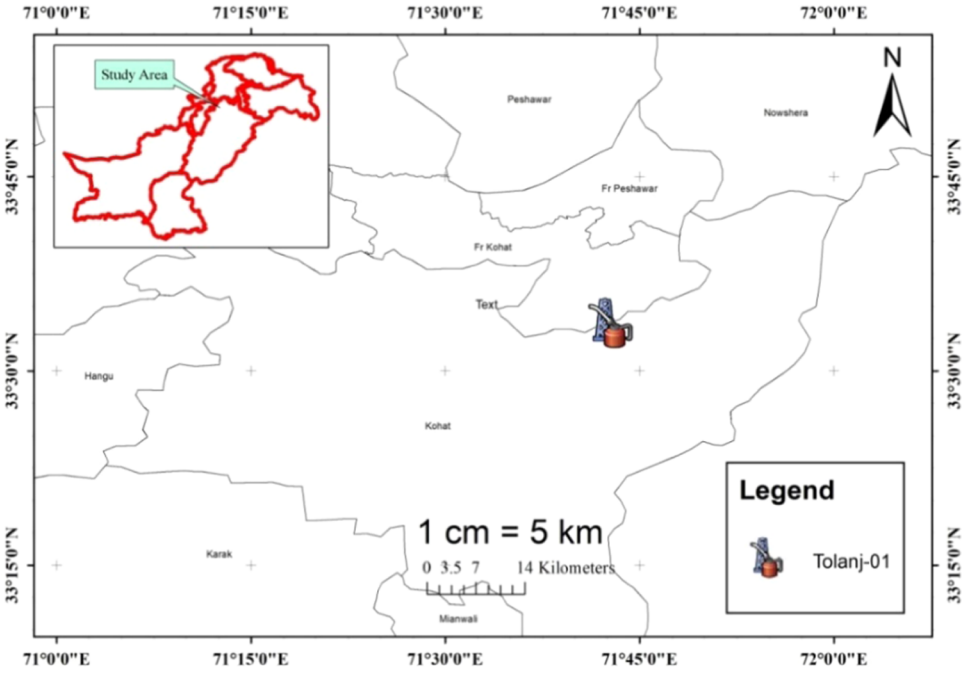

Figure 1. Inset map showing the location of the study area, Kohat District, Pakistan, and the location of the Tolanj-01 well.

methylphenanthrene index (MPI-1) values, Moretane index, and Pr/*n*-C_{17} vs Ph/*n*-C_{18} plots also show higher thermal maturity for these rock extracts.

1. INTRODUCTION

Products obtained from petroleum are primarily used as energy sources. Technological advancements and increased demand for fossil fuels have led to a growing trend in petroleum exploration.[1−3] Currently, the economy is heavily reliant on the energy sector and the amount of energy that is utilized. The success of global economy largely dependst on energy sources, particularly electricity, and availability. A country's economic and political stability also hinges on the energy sector, particularly the exploration and availability of hydrocarbons, which are essential for development, prosperity, and nation building.[4−6]

Energy demand is rapidly increasing, and is expected to grow by 41% from 2012 to 2035.[7] This demand is driven by factors, such as population growth and the rapidly expanding automotive industry. As energy demand continues to increase, there is a growing demand for fossil fuels. However, the past few years have seen a significant decrease in oil prices due to the financial crisis and unstable world markets. Despite this, continuous research is needed to explore fossil fuels in order to meet the future needs for oil and natural gas.

Understanding the economic significance of the petroleum system is crucial. This system involves accumulating, transforming, and migrating organic matter into a reservoir over sufficient geologic time and under proper burial depth and temperature−pressure conditions. The economic viability of a petroleum system depends on factors such as the quality, quantity, and type of petroleum present.[8−11] The search for oil focuses on identifying porous and permeable formations, commonly called source or reservoir rock. The first stage of the exploration process involves geochemical evaluation of the source rock. This evaluation provides valuable insights into the organic matter, thermal maturity, age, environment of deposition, kerogen type, and production potential of the source rock.[12−15]

Pakistan has significant potential for hydrocarbons, and the Kohat Basin has emerged as a profitable hydrocarbon-bearing province in the country. This area has gained attention for oil and gas exploitation due to the successful exploitation of oil and gas reserves in the Potwar Plateau. The presence of diapiric structures, oil seeps, and shale oil on the Kohat Plateau makes it an attractive area for further investigation and exploitation. The exploration of the Kohat Basin has been ongoing for several decades, but the thick Siwalik formation has posed challenges to the development of oil fields in the area. However, recent discoveries such as the Nashpa and Mela fields have increased Pakistan's hydrocarbon reserves over the past 15 years. In the early days of exploration, the focus was primarily on reservoir properties, but now it has shifted toward source rocks and the origin of hydrocarbons. Unfortunately, Pakistan lacks the technology and resources needed to explore unconventional reservoirs efficiently. This research could aid oil companies in future exploration ventures involving unconventional reservoirs.[13,16,17]

In the past, most evaluations were done with the help of surface geology, which is less reliable. However, with the advancement of geophysics, seismic studies have helped geologists to predict more about subsurface possibilities. Recently, the importance of geochemistry has been understood widely around the globe, as it helps in understanding and exploring the origin of hydrocarbons and petroleum. Paleocene-aged rocks are considered to be source rocks that have the potential for generation in the Kohat Sub-Basin and Potwar Sub-Basin.[17] Previous research in the Kohat-Potwar Basin in North Pakistan has identified numerous source rocks that have the potential for hydrocarbons, including the Salt Range formation

https://doi.org/10.1021/acsomega.3c09457
ACS Omega 2024, 9, 14123−14141

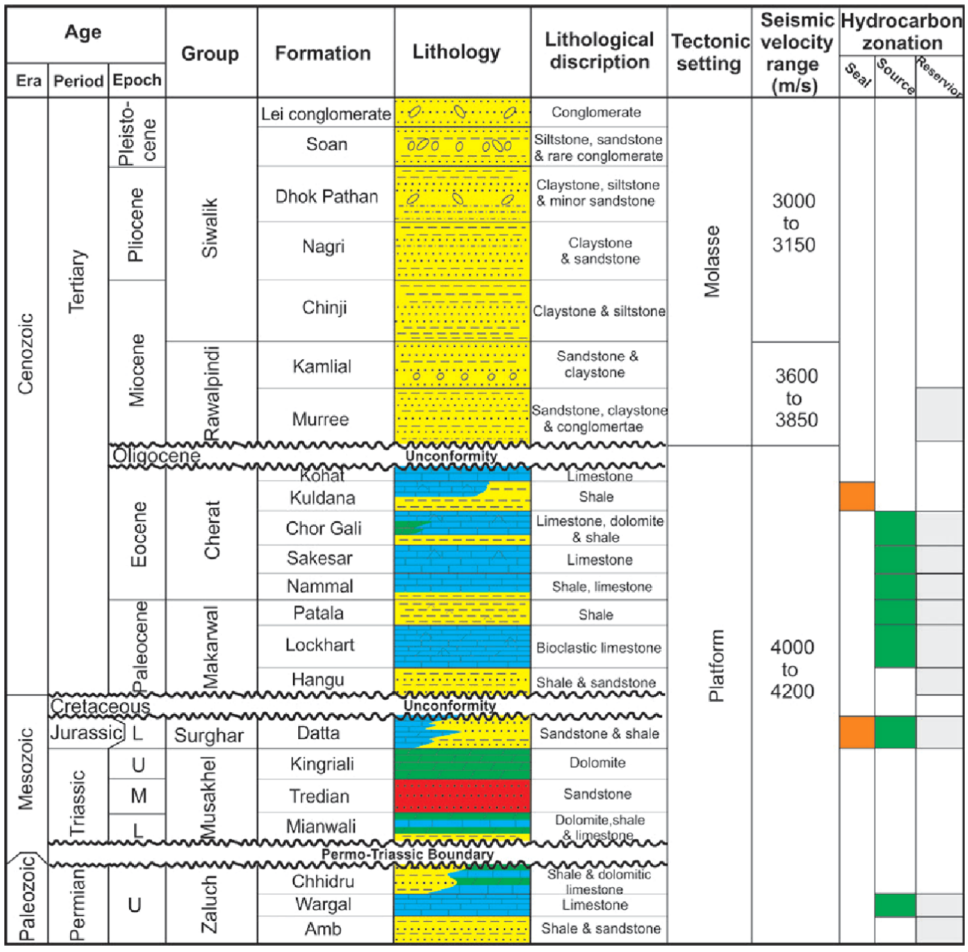

Figure 2. Generalized stratigraphic column of the Kohat sub-basin (adopted from ref 17).

(Precambrian), the Dandot, Sardhai, and Chidru formations (Permian), and the Lockhart Limestone and Patala formations (Paleocene).[18−20] The total organic content (TOC) ranges from 0.5 to less than 3.5%. Hydrocarbons are considered to be generated from the source rocks with Types II and III kerogen.[21] As per detailed geochemical analysis, the Patala formation in the Kohat-Potwar Plateau has good shale gas potential.[13] Previous studies have shown that the Paleocene-aged source rocks in the Kohat Sub-Basin have good to excellent hydrocarbon generation potential, making it a promising target for exploration and production activities.

Extensive research has been carried out on different aspects, such as surface geology, biostratigraphy, sedimentology, hydrocarbon prospect interpretation via petrophysical analysis, seismic studies, and reservoir evaluation of Paleocene-aged formations in the Kohat sub-basin.[19] However, comparatively limited research has been done on the source rock evaluation of Paleocene-aged formations in the Kohat sub-basin. This research focuses on determining the geochemical evaluation of source rocks of Paleocene age in the Tolanj-01 well, Kushal Garh Block, and Kohat sub-basin. This work will help to better understand the source rocks in Tolanj-01 and improve the knowledge of petroleum prospects for scientific and economic interests.

2. LOCATION OF THE STUDY AREA AND GEOLOGICAL SETTING

The study area of the Tolanj-01 well is located in the Upper Indus Basin, Kushal Garh Block, Kohat District, KPK, Pakistan. The Tolanj-01 well lies approximately 150 km SW of Islamabad. It is easily accessible through the M1 and M2 motorways and the N-80 Highway. It is about 20 km from the Dakhni Oil and Gas Field in the southeast and 20 km from Shekhan-01 in the Northwest. The latitude (33° 33′ 42″) and longitude (71° 42′ 50″) of the study area and Tolanj-01 well are shown in the location map (Figure 1).

The Tolanj-01 well was drilled by AMOCO (APEC) in 1991. The Kohat area is bounded by the main boundary thrust (MBT) to the North and by Trans Indus Ranges to the South. The Kohat Plateau merges to the southwest with the Bannu Basin. The eastern limit of the Kohat Plateau is marked by the River Indus, which distinguishes it from the Potwar Plateau, and in the west, the Kohat Plateau is restricted by the NNE-SSW-oriented Kurram fault. The Kohat−Potwar Basin is present in northern Pakistan, located between latitude 32° and 34° N and longitude 70° and 74° E. The Kohat area is bounded by the MBT to the north and by Trans Indus Ranges to the south. The Kohat Plateau merges southwest with the Bannu Basin. The River Indus points to the Kohat plateau's eastern limit, distinguishing it from the Potwar plateau, and in the west, the Kohat plateau is restricted by the NNE-SSW-oriented Kurram fault.

The surface and subsurface outcrops of the area below the Lower Eocene appear less deformed and distorted than those of

https://doi.org/10.1021/acsomega.3c09457
ACS Omega 2024, 9, 14123−14141

Table 1. Sample Description of the Target Well

depth (ft)	formation	lithology	TOC (wt %)	S1 (mg/g)	S2 (mg/g)	S3 (mg/g)	T_{max} (°C)	GP (mg HC/g rock)	HI (mg HC/g TOC)	OI (mg CO_2/g TOC)	PI ($S_1/(S_1 + S_2)$)
4705	Patala	Shale	0.28	0.08	0.22	0.05	450	0.3	79	1	0.27
4850			0.29	0.16	0.24	0.13	449	0.4	83	4	0.4
4905			0.38	0.14	0.35	0.12	451	0.49	92	5	0.29
5005			0.35	0.13	0.25	0.21	452	0.38	71	7	0.34
5110			0.23	0.07	0.15	0.12	449	0.22	65	3	0.32
5205			0.18	0.05	0.21	0.19	447	0.26	117	3	0.19
5305			0.41	0.13	0.35	0.29	450	0.48	85	12	0.27
5405			0.27	0.06	0.15	0.06	451	0.21	56	2	0.29
5535			0.22	0.07	0.15	0.12	446	0.22	68	3	0.32
5605			0.16	0.1	0.27	0.21	445	0.37	169	3	0.27
5705			0.11	0.11	0.25	0.06	366	0.36	227	1	0.31
5805			0.19	0.11	0.31	0.07	413	0.42	163	1	0.26
5905			0.2	0.13	0.29	0.07	358	0.42	145	1	0.31
6150			0.24	0.13	0.29	0.07	451	0.42	121	2	0.31
6300			0.76	0.1	0.13	0.3	455	0.23	17	23	0.43
6405			0.81	0.31	0.49	0.06	458	0.8	60	5	0.39
6505			0.76	0.31	0.42	0.18	457	0.73	55	14	0.42
6705			0.18	0.05	0.16	0.19	459	0.21	89	3	0.24
6815			0.15	0.05	0.15	0.21	455	0.2	100	3	0.25
7010			0.31	0.08	0.17	0.11	456	0.25	55	3	0.32
7305			0.14	0.08	0.19	0.19	455	0.27	136	3	0.3
7405			0.13	0.07	0.18	0.18	360	0.25	138	2	0.28
7605			0.18	0.05	0.15	0.21	336	0.2	83	4	0.25
7745			0.17	0.09	0.21	0.11	458	0.3	124	2	0.3
7850			0.13	0.13	0.27	0.12	413	0.4	208	2	0.33
7950			0.18	0.2	0.24	0.33	456	0.44	133	6	0.45
8015	Lockhart		0.29	0.19	0.24	0.33	460	0.43	83	10	0.44
8035			0.47	0.24	1.1	0.13	458	1.34	234	6	0.18
8150			0.27	0.19	0.25	0.74	419	0.44	93	20	0.43
8205			0.51	0.16	0.7	0.44	455	0.86	137	22	0.19
8230			0.47	0.07	0	0.21	461	0.07	0	10	1
8250		Limestone	0.37	0.05	0	0.16	416	0.05	0	6	1
8265			0.47	0.1	0.44	0.26	458	0.54	94	12	0.19
8280			0.43	0.05	0	0.29	416	0.05	0	12	1
8350			0.05	0.07	0.05	0.04	460	0.12	100	0	0.58
8326			0.47	0.08	0.01	0.32	339	0.09	2	15	0.89
8370			0.12	0.08	0.04	0.19	337	0.12	33	2	0.67
8390			0.68	0.12	0.51	0.27	450	0.63	75	18	0.19
8400	Hangu	Shale	0.2	0.08	0.12	0.12	459	0.2	60	2	0.4
8420			0.75	0.13	0.39	0.63	456	0.52	52	47	0.25
8440			0.95	0	0	0	458	0	0	0	0
8460			1.2	0.07	0.44	0.03	455	0.51	37	4	0.14
8468			0.82	0.19	0.57	0.11	469	0.76	70	9	0.25
8472			1.56	0.27	1.09	0.15	473	1.36	70	23	0.2
8477			0.62	0.17	0.39	0.14	473	0.56	63	9	0.3
8490			0.76	0.16	0.17	0.15	458	0.33	22	11	0.48
8500			0.65	0.23	0.42	0.13	468	0.65	65	8	0.35
8515			1.65	0.06	0.32	0.24	468	0.38	19	40	0.16
8526			1.58	0.37	0.68	0.46	463	1.05	43	73	0.35
8540			0.76	0.29	0.08	0.11	467	0.37	11	8	0.78
8560			0.28	0.25	0.51	0.79	453	0.76	182	22	0.33
8584			4.49	0.9	4.06	0.08	465	4.96	90	36	0.18
8600			0.34	0.11	0.16	0.83	471	0.27	47	28	0.41
8620			1.86	0.02	0.43	0.05	470	0.45	23	9	0.04
8700			0.61	0.1	0.03	0.69	467	0.13	5	42	0.77
8750			0.08	0.12	0.08	1.43	410	0.2	100	11	0.6

the Eocene. The entire Kohat-Potwar region comprises Imbricate Wrench Faults, which are steep in Kohat and gentle in the Potwar region.[22] This basin has rocks from the Eocene to Pliocene age. Below the Paleocene, Mesozoic rocks are present. The southern side comprises Miocene to Pliocene strata, which are thrusting southward along with the direction of Bandarbarra

https://doi.org/10.1021/acsomega.3c09457
ACS Omega 2024, 9, 14123−14141

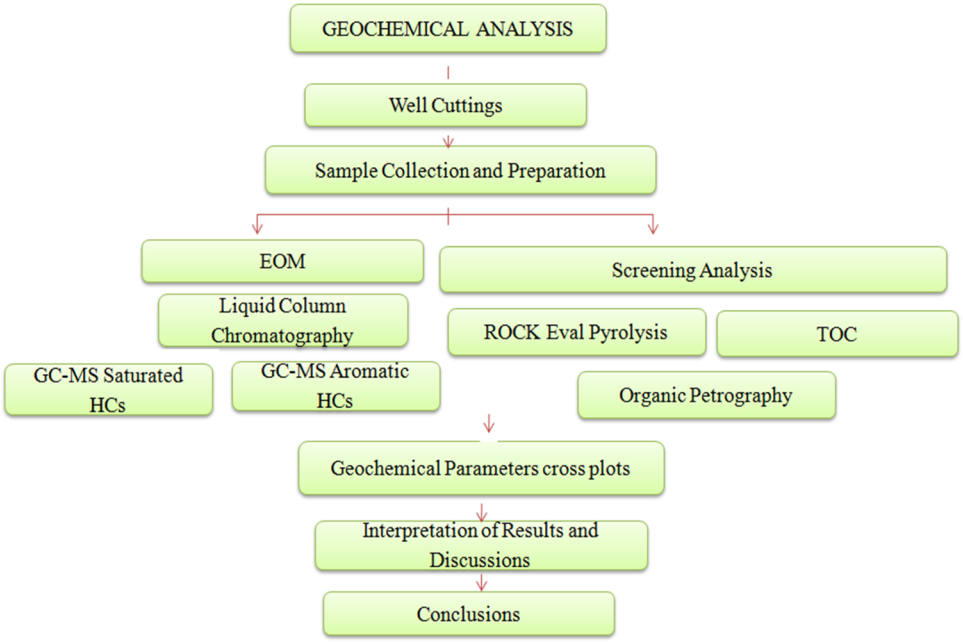

Figure 3. Methodology adopted for geochemical analysis.

and Karak Thrust on Bannu Depression; Pliocene to Pleistocene sequences are present at the western side and the Potwar plateau are present at the Eastern side. The southern side of the Kohat-Potwar Basin, an area with sediment ranges from Paleozoic to Recent, is relatively flattering with dips of monoclines in the north direction.[23]

The burial record of the Kohat-Potwar fold and thrust belts occurred in the Precambrian age by sediment deposition in the Salt Range formation and Jhelum Group (Figure 2). Upper Cambrian, Ordovician, Silurian, Devonian, or Carboniferous strata are absent in this basin because of nondeposition and/or erosion.[24] A unit of rock generates oil and gas for commercial accumulations. Common source rocks are shale and limestone. Infra Cambrian Salt Range Formation displays good TOC and very good hydrogen index (HI) values indicative of type II organic matter, Organic-rich shales of Mianwali and carbonates of Kingriali formations (Triassic), Datta formation (Jurassic) and Chichali (Cretaceous) are considered as potential source rocks in the area. The Patala shales (Paleocene) are a proven source in the Upper Indus Basin. Maturity modeling suggests that the Paleocene and older source rocks contain oils to condense the maturity levels in the area. The main source potential lies in the Datta (excellent TOC values, type II/III kerogen), Chichali, and Lumshiwal formations, which have been proven to yield in surrounding wells. In the eastern part of Potwar, the Patala formation and Lockhart Limestone are confirmed and demonstrated as source rocks for high-quality oil.[14,21]

3. MATERIALS AND METHODS

Fifty-six (56) samples of well cuttings of Paleocene rock units from the Tolanj-01 well were obtained to analyze the potential source rock, organic matter maturity, and biomarker characterization (Table 1). Geochemical analysis was conducted at the Hydrocarbon Development Institute of Pakistan (HDIP) Laboratory. The techniques include assessment of total organic carbon (TOC), Rock-Eval pyrolysis, organic petrography (vitrinite reflectance), column chromatography, and gas chromatography−mass spectrometry (GC−MS; Figure 3).[25,26] The TOC (wt %) analysis and Rock-Eval pyrolysis studies were performed on 18 (18) samples of the Hangu formation, 12 (12) samples from the Lockhart formation, and 26 (26) samples from the Patala formation. An organic petrography (vitrinite reflectance, R_0) assessment was performed on a drill-cutting sample of each Paleocene rock unit from the Tolanj-01 well.[27] The biomarker analysis was conducted on three source rock extracts (EOM) from drill cuttings of the Paleocene rock units in total by taking one sample from each unit.

The CS-300 (LECO) analyzer and Rock-Eval pyrolysis-6 instruments were utilized to estimate the total organic carbon content (TOC, wt %) and Rock-Eval parameters, respectively.[28] Rock-Eval analysis includes the assessment of volatile hydrocarbons at 300 °C (S_1), remaining hydrocarbons after pyrolysis of kerogen (S_2), the amount of CO, CO_2 generated by pyrolysis (S_3), temperature at peak evolution of S_2 hydrocarbons (T_{max}), hydrogen index (HI = S_2/TOC × 100), oxygen index (OI = S_3/TOC × 100), production index (PI = S1/S_1 + S_2), and genetic potential (GP = S_1 + S_2).[29,30] Furthermore, these parameters and plots were used to determine the source rock potential, kerogen type, and thermal maturity of the Paleocene formations from drill cuttings. Organic petrographic studies were conducted on prepared pellets of samples from a single sample of each Paleocene formation under white and blue light using a Zeiss Axio microscope (Z1M). A Soxhlet extractor was used further to extract bitumen (EOM) from the drill cuttings using conventional dichloromethane/methanol solvents. The bitumen was fractionated into saturated, aromatic, nitrogen, sulfur, and oxygen (NSO) compound fractions in a glass column filled with silica slurry and alumina using column chromatography. The chromatograms obtained from gas chromatography−mass spectrometry (GC-MS) were used to conduct biomarker analysis of the extracted organic matter from three drill cuttings of Paleocene rock units present in the Tolanj-01 well. GC-MS was mainly applied to identify steroids and terpenoids, which are usually present in trace quantities. Different geochemical parameters such as thermal maturity, origin of organic matter,

https://doi.org/10.1021/acsomega.3c09457
ACS Omega 2024, 9, 14123−14141

kerogen type, age, and environment of deposition were determined from the resultant chromatograms.[31]

4. RESULTS

4.1. Organic Richness and Rock-Eval Pyrolysis. The results of organic richness and Rock-Eval pyrolysis were

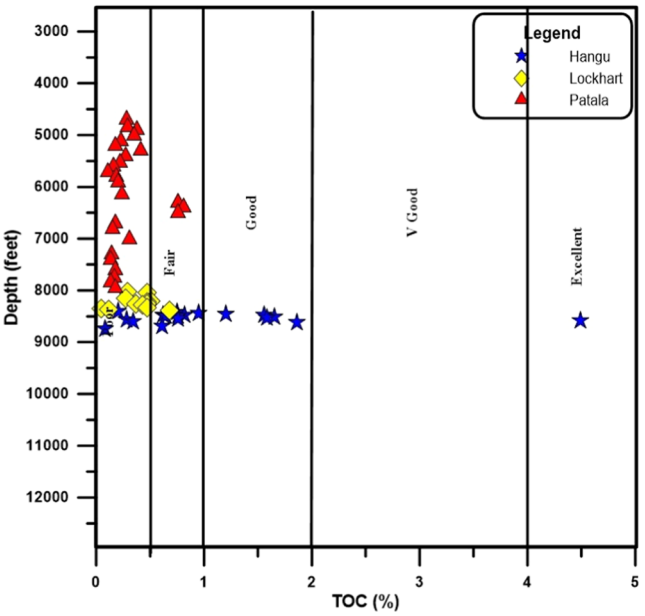

Figure 4. TOC vs depth plot for Hangu, Lockhart, and Patala formations.

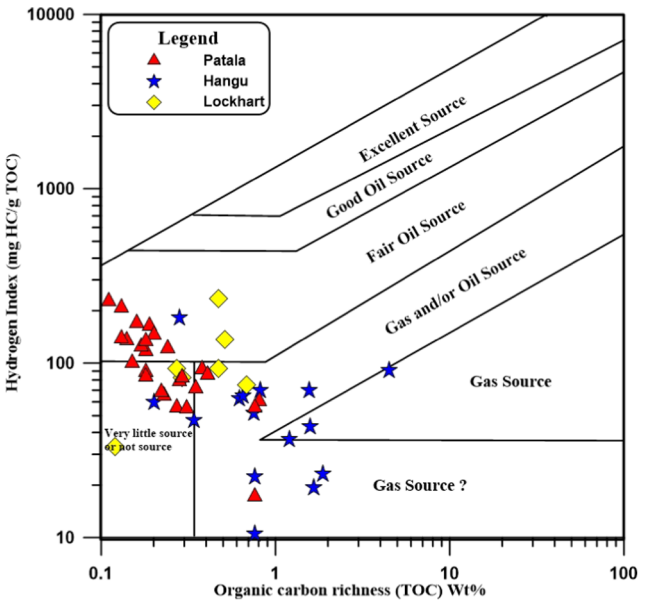

Figure 5. HI vs TOC plot for the Hangu, Lockhart, and Patala formations.

obtained for 56 (56) samples, including 18 (18) samples of the Hangu formation, 12 (12) samples of the Lockhart formation, and 26 (26) samples of the Patala formation (Table 1). The estimated TOC values of Patala, Lockhart, and Hangu formations from well cuttings lie in the ranges 0.11−0.81, 0.05−0.68, and 0.08−4.49 wt %, respectively. The TOC values for shale samples of the Hangu formation fall in the category of

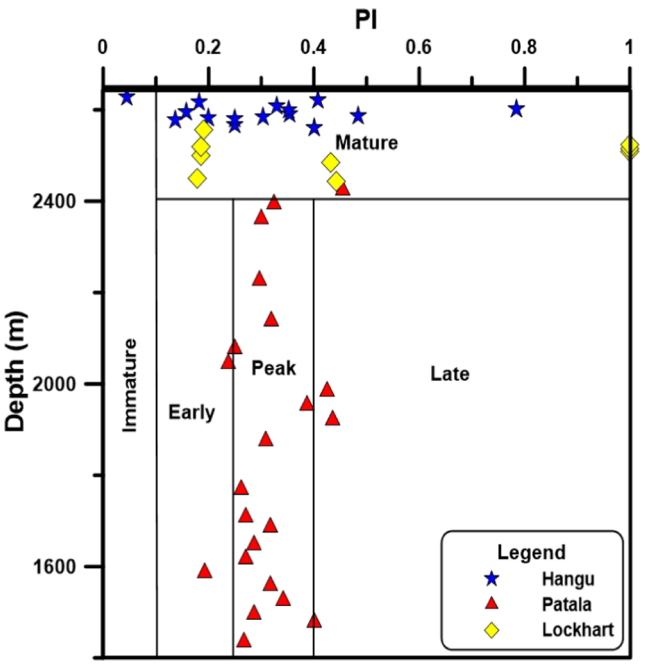

Figure 6. PI vs depth plot for the Hangu, Lockhart, and Patala formations.

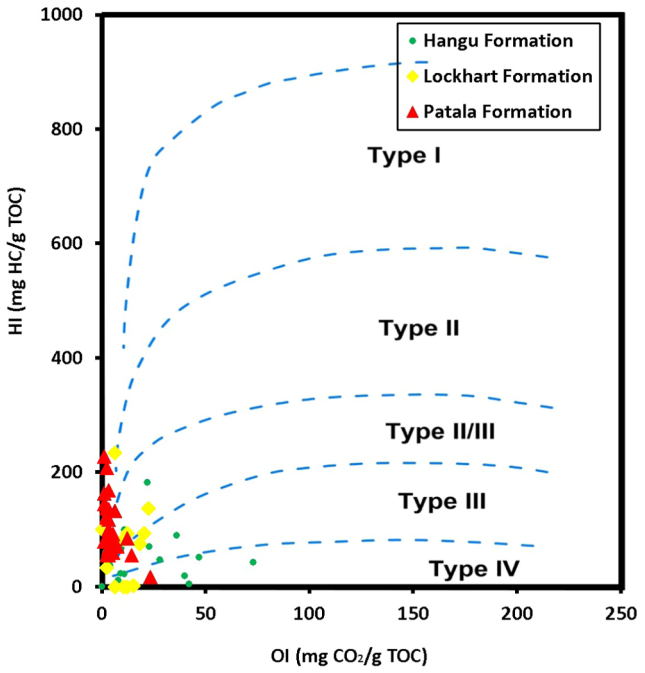

Figure 7. HI vs OI plot for the Hangu, Lockhart, and Patala formations.

poor to good, while those for limestone samples of the Lockhart formation belong to the poor to fair zone. In the shale samples from Patala formation, the TOC values lie within the plot's poor to fair zone (Figure 4). The TOC values at present do not reflect the original or total organic matter because over time and with the increase in thermal maturity, kerogen is converted into hydrocarbons, and the value of TOC decreases.

The Rock-Eval pyrolysis study reveals that S_1, S_2, S_3, and T_{max} values for the shale cuttings of Patala formation ranged from 0.05 to 0.31 mg/g, 0.13 to 0.49 mg/g, 0.05 to 0.33 mg/g, and 336−459 °C, respectively. The results for the limestone cutting

https://doi.org/10.1021/acsomega.3c09457
ACS Omega 2024, 9, 14123−14141

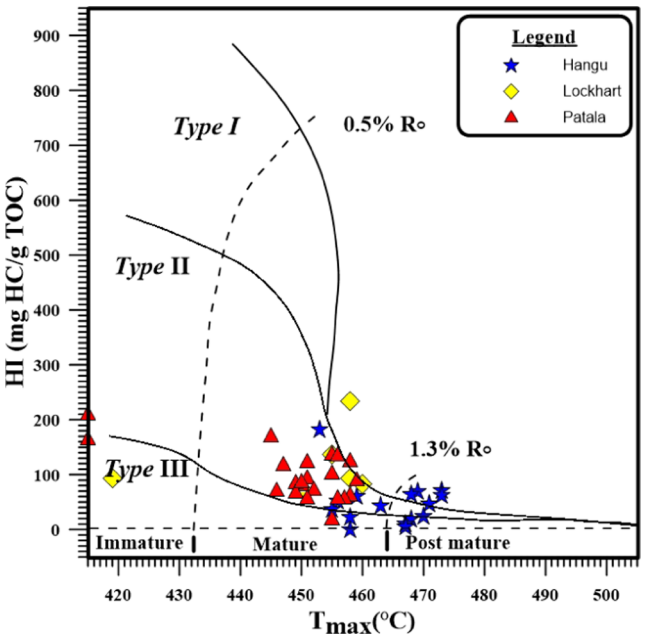

Figure 8. HI vs Tmax plot for the Hangu, Lockhart, and Patala formations.

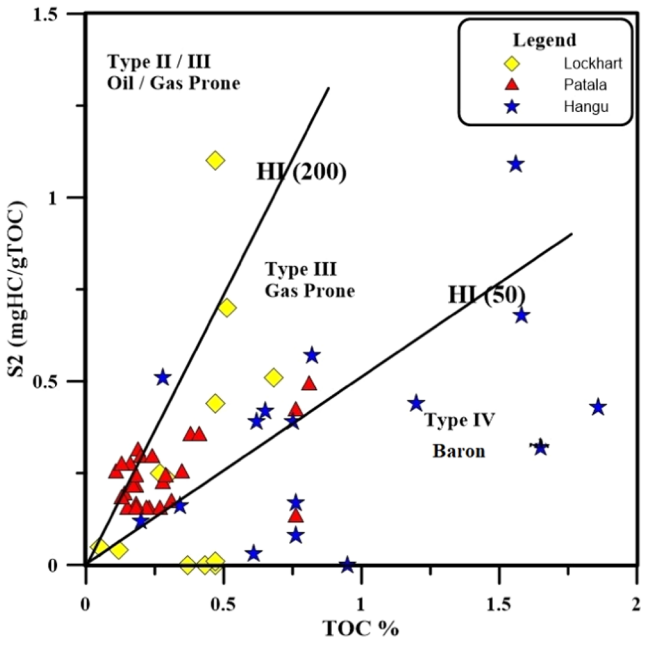

Figure 9. S_2 vs TOC plot for the Hangu, Lockhart, and Patala formations.

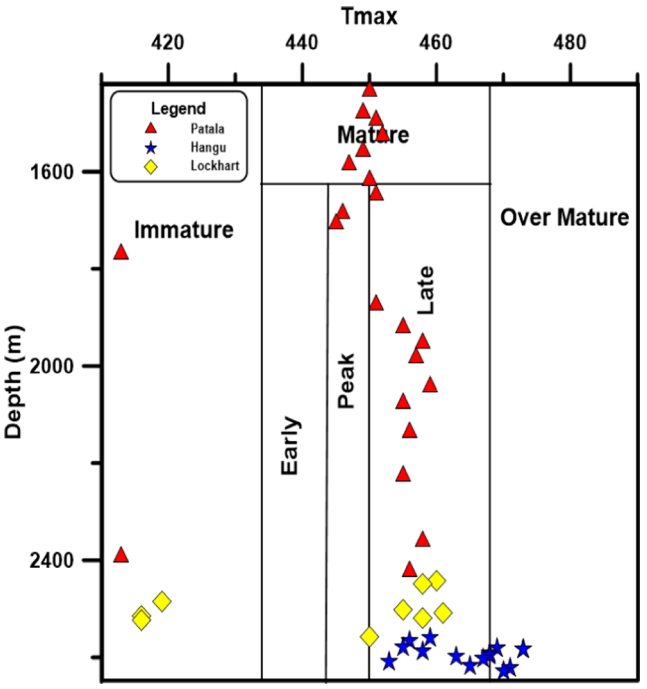

Figure 10. T_{max} vs depth for the Hangu, Lockhart, and Patala formations.

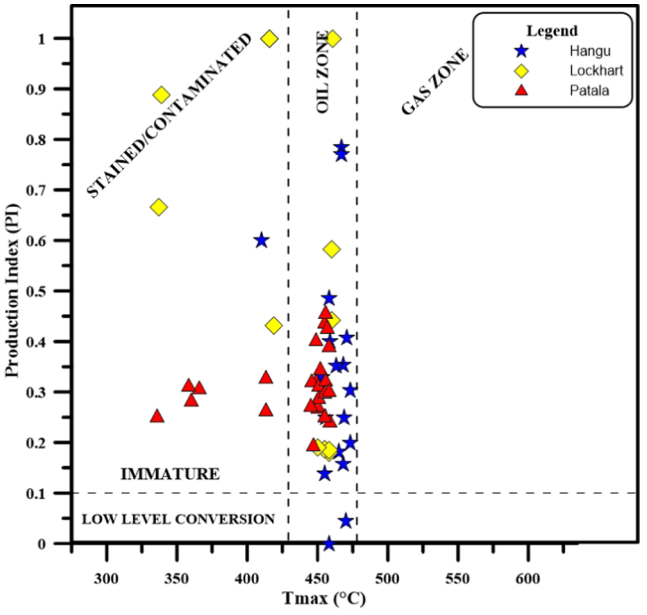

Figure 11. PI vs T_{max} plot for all three formations.

samples of the Lockhart formation show that S_1, S_2, S_3, and T_{max} values range from 0.05 to 68 mg/g, 0.05 to 0.24 mg/g, 0−1 mg/g, and 337−461 °C, respectively. On the other hand, shale cuttings of the Hangu formation show S_1, S_2, S_3, and T_{max} in the ranges 0−0.9 mg/g, 0−4.06 mg/g, 0−1.43 mg/g, and 410−473 °C, respectively. The values of hydrogen index (HI) and oxygen index (OI) for the Patala and Lockhart formations are not too high and range between 17−227 mg HC/g, 1−23 mg CO_2/g, 0−234 mg HC/g, and 0−22 mg CO_2/g, respectively. The estimated average genetic potential (GP) for the studied samples for the Patala, Lockhart, and Hangu formations are 0.36, 0.40, and 0.75 mg HC/g, while the average respective production index (PI) values of these rock units are 0.31, 0.56, and 0.33, respectively. The estimated geochemical parameters were further utilized to obtain various plots (Figures 5−12) to determine the source rock potential of the Paleocene units of the basin. The plot between HI and TOC reveals that the organic matter in both the Patala and Lockhart formations has a potential to generate oil and gas, whereas the Hangu formation has a potential for gas generation (Figure 5).[32,33]

Maturation stages were defined for the Paleocene units on the basis of the PI−depth plot, which clearly indicates that the Patala formation shows a peak stage of hydrocarbon generation. In contrast, the other two rock units belong to the mature hydrocarbon generation stage (Figure 6).

https://doi.org/10.1021/acsomega.3c09457
ACS Omega 2024, 9, 14123−14141

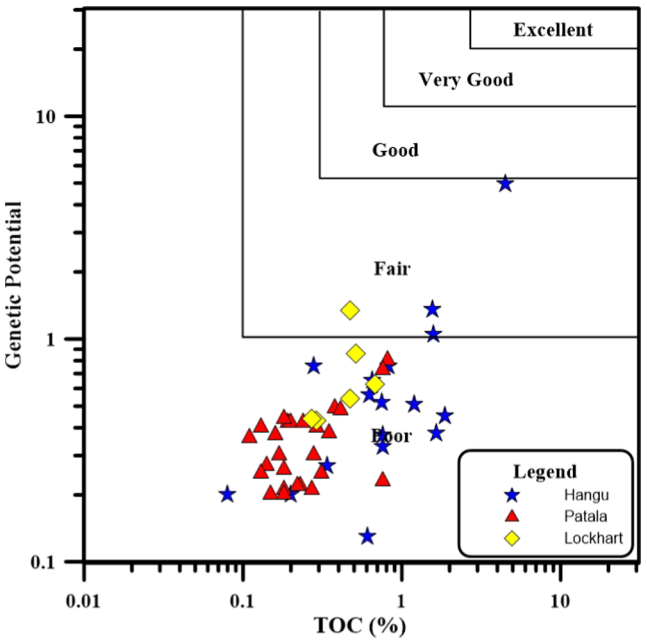

Figure 12. GP vs TOC plot for the Hangu, Lockhart, and Patala formations.

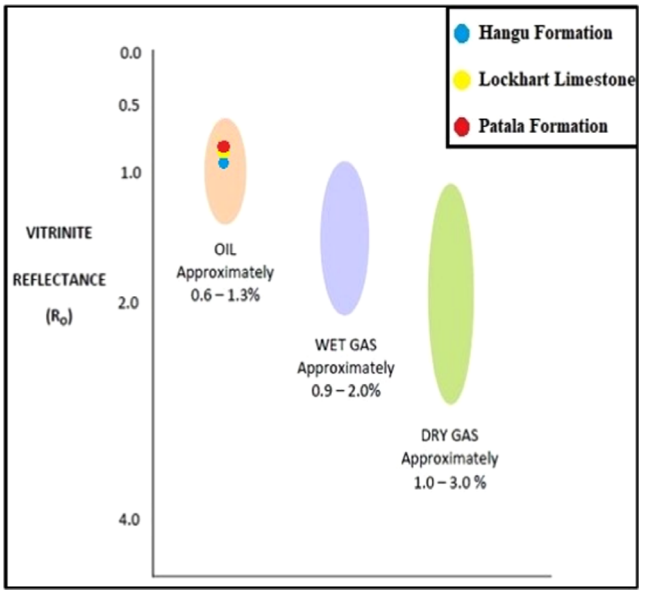

Figure 13. Vitrinite reflectance values show transformation into hydrocarbon types with increasing thermal maturity (modified from ref 35).

Table 2. Vitrinite Reflectance Values of Well Cuttings from Tolanj-01

formation	no. of samples	R_0 (%)
Hangu formation	01	0.95
Lockhart formation	01	0.89
Patala formation	01	0.82

Several plots were constructed to delineate the kerogen type, including HI as a function of OI, HI vs T_{max}, and S_2 vs TOC plots (Figures 7–9).

The obtained plots show that all Paleocene formations fall into the category of Type-III kerogen (gas-producing). The thermal maturity of the Paleocene rocks was studied using plots of T_{max} vs depth and PI vs T_{max}. The plot of T_{max} vs depth indicates that the Lockhart and Hangu formations are thermally mature and fall into the category of the late oil window. At the same time, the Patala formation bears a lower thermal maturity and falls in the peak to the late oil window (Figure 10).

Similarly, the plot of PI vs T_{max} also shows that the majority of the values of the Paleocene units fall in the oil window category, except for a few values that fall in the immature region and show oil staining/contamination (Figure 11). The plot of the genetic potential (GP) vs TOC was also constructed to rank source rock productivity. This indicates that all of the Paleocene formations in the study area have poor genetic potential, except for a few samples of Hangu and Lockhart formations (Figure 12).

4.2. Organic Petrography. The stage of catagenesis at the onset of oil generation, also known as the oil window, is represented by 0.6–1.3% R_0. As the temperature increases, the increase in thermal cracking forms the condensates (wet gas), with R_0 values of 1.3–2%. R_0 values of 2–3% show the dry gas phase, while values greater than 3% show that the source rock is spent, has already produced all the hydrocarbons, and does not possess enough hydrogen to produce further hydrocarbons.[34] Vitrinite reflectance shows the transformation stage of the organic matter and gives an idea of the type of hydrocarbon formed (Figure 13). In the present study, one sample from the drill cuttings of the Paleocene unit was used to perform organic petrography. The polished particulate pellets prepared were studied under white and blue light using a Z1M Zeiss microscope. Vitrinite reflectance standards of 0.589, 0.907, and 1.711% were used to calibrate the microscope. The estimated values of vitrinite reflectance (R_0) for these formations are 0.82, 0.89, and 0.95% for the Patala, Hangu, and Lockhart formations, respectively (Table 2).

All of these Paleocene units in the study area fall in the category of the mature oil window, where values of vitrinite reflectance for the Patala Formation are the least due to the shallower depth of the formation compared to the rest of the formations. These results are quite consistent with the results obtained from Rock-Eval pyrolysis (T_{max}), which also indicates that Paleocene formations bear the potential to generate oil and gas. This phase of thermal maturity corresponds to subsurface temperature in the range of 90–150 °C and oil window.

4.3. Biomarkers Studies. Biomarkers are compounds found in a variety of materials such as oil, rock units, soil extracts, and recent sediments, which can be related to organic molecules present in living organisms during that time. Biomarkers such as terpenes, steranes, isoalkanes, and *n*-alkanes dominate during the oil window phase of catagenesis, while their concentrations are extremely low in condensate or wet gas. The presence of these compounds is particularly useful for

Table 3. Hydrocarbon Classes and Biomarkers Used for Sample Analysis

biomarker	fragmentogram/mass/charge ion chromatograms (m/z)
n-alkanes	57
pristane and phytane	183
aromatic hydrocarbons	178, 184, 192
tricyclic terpanes	191
hopanes	191
homohopanes	191
regular steranes	217, 218

https://doi.org/10.1021/acsomega.3c09457
ACS Omega 2024, 9, 14123–14141

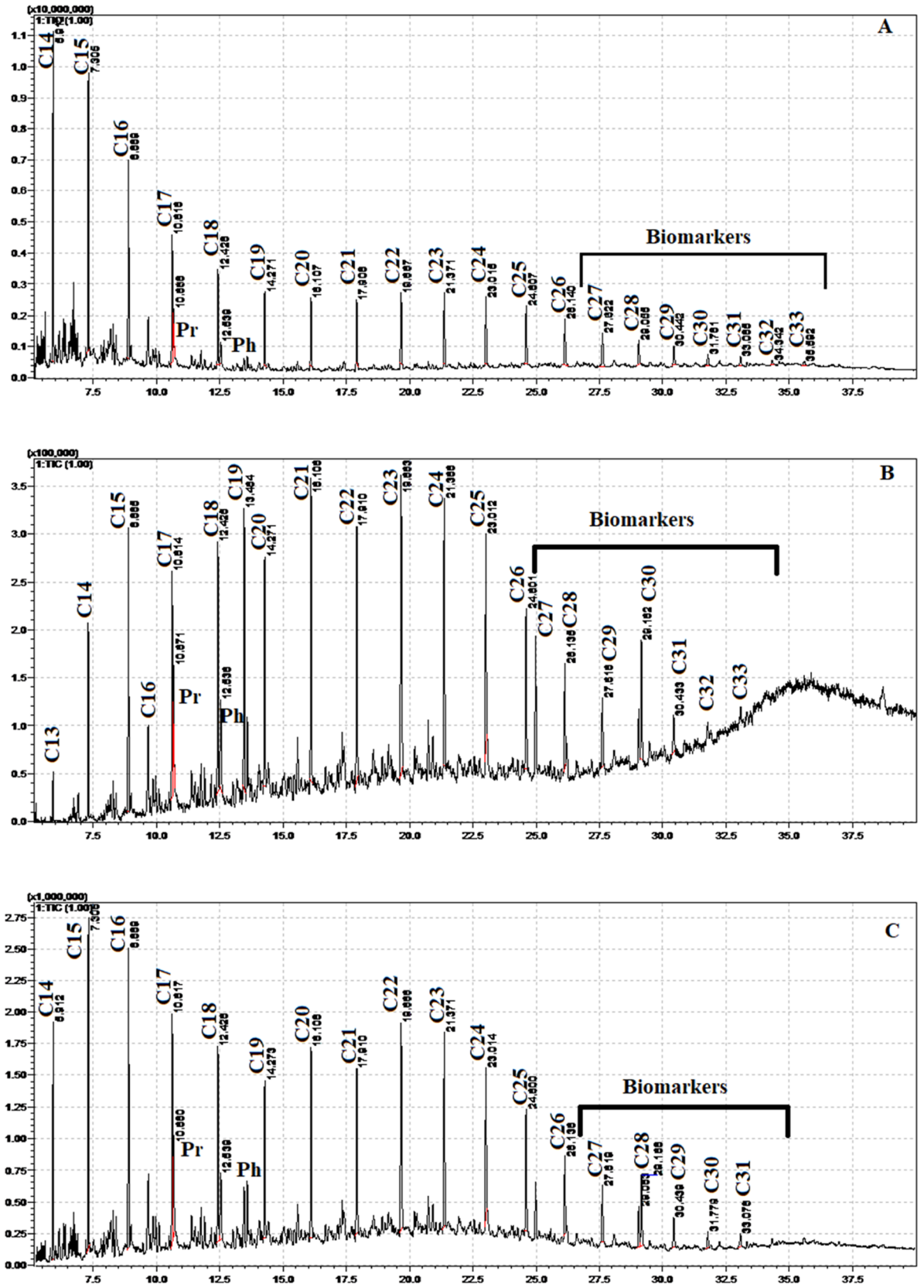

Figure 14. Chromatograms of saturated fractions of (A) Patala formation, (B) Lockhart Limestone, and (C) Hangu formation.

geoscientists to understand the depositional environment and their biological involvement in hydrocarbon generation.[30,36] Additionally, the stable molecular structure of these compounds can be quite helpful in studying the input source of the organic matter, biodegradation level, lithology of the source rock, effects of changes in thermal maturity during catagenesis, etc.[37,38] In the present study, one sample from drill cuttings of each Paleocene unit similar to Rock-Eval pyrolysis was selected to analyze

https://doi.org/10.1021/acsomega.3c09457
ACS Omega 2024, 9, 14123−14141

Table 4. Parameters Derived from *n*-Alkanes of Source Rock Extracts[a]

parameter	Patala	Lockhart	Hangu
TAR	0.10	0.26	0.12
CPI_1	1.04	0.91	0.95
OEP_1	1	0.92	0.95

[a]Terrigenous aquatic ratio (TAR): $(nC_{27} + nC_{29} + nC_{31})/(nC_{15} + nC_{17} + nC_{19})$; carbon preference Index (CPI_1): $2(C_{23} + C_{25} + C_{27} + C_{29})/C_{22} + 2(C_{24} + C_{26} + C_{28}) + C_{30}$; Odd to even predominance (OEP_1): $(C_{21} + 6C_{23} + C_{25})/(4C_{22} + 4C_{24})$.

Table 5. Parameters Derived from Isoprenoids of Source Rock Extracts[a]

parameter	Patala	Lockhart	Hangu
Pr/Ph	1.8	1.23	1.33
Pr/*n*-C_{17}	0.44	0.64	0.50
Ph/*n*-C_{18}	0.30	0.54	0.42

[a]Pr: pristane; Ph: phytane; *n*-C_{17}: C_{17} normal alkane, and *n*-C_{18}: C_{18} normal alkane.

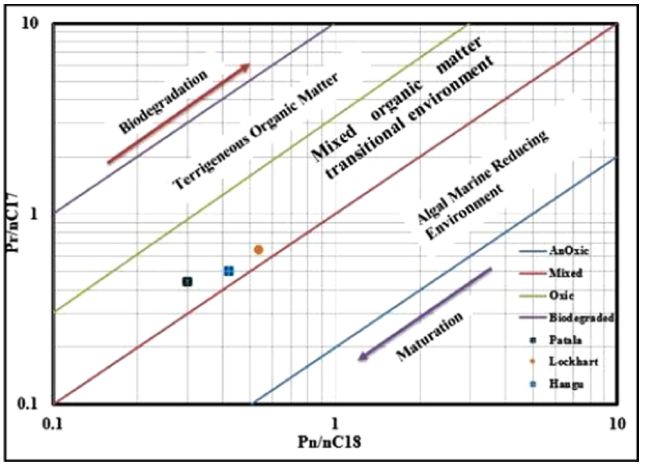

Figure 15. Plot of Pr/*n*-C_{17} vs Ph/*n*-C_{18} ratios for Hangu, Lockhart, and Patala source rock extracts.

biomarkers present in the rock extracts. The saturated and aromatic hydrocarbons were analyzed by using GC-MS (Table 3).

4.3.1. Distribution of n-Alkanes and Isoprenoids. The biomarker studies of the three (3) samples from Paleocene units reveal that *n*-alkanes range between C_{13} and C_{33} (Figure 14).

Table 7. Biomarker Derived from Regular Steranes[a]

parameters	Patala	Lockhart	Hangu
C_{27} (%)	35	25	29
C_{28} (%)	31	26	22
C_{29} (%)	34	51	50
$C_{29}\beta\beta/(C_{29}\beta\beta + C_{29}\alpha\alpha)$	0.51	0.51	0.50
$C_{29}S/C_{29}S + C_{29}R$	0.50	0.49	0.50
C_{28}/C_{29}	0.91	0.50	0.44
C_{29}/C_{27}	0.9	2.04	1.72

[a]Percentages of C_{27}, C_{28}, and C_{29}.Steranes: $C_{29}\beta\beta/(C_{29}\beta\beta + C_{29}\alpha\alpha)$; $C_{29}S/C_{29}S + C_{29}R$, C_{28}/C_{29}, C_{29}/C_{27}.

Table 8. Geochemical Parameters Derived from Aromatic Hydrocarbons[a]

parameters	Patala	Lockhart	Hangu
MPI-1	1.083	1.195	1.143
MPI-3	0.941	1.10	1.263
Rc%	1.049	1.117	1.085
MPR-1	2.02	2.35	2.66

[a]Methylphenanthrene index (MPI-1): 1.5 × (3MP + 2MP)/(P + 1MP + 9MP); methylphenanthrene index (MPI-3): (3 + 2MP)/(1MP + 9MP); Rc%: 0.6 × MPI-1 + 0.4; MPR-1: 2MP/1MP.

The higher concentrations of short-chain alkanes compared to longer-chain alkanes in the rock extracts of the Patala, Lockhart, and Hangu formations are associated with the marine source input.[39] These short-chain alkanes are generally produced by benthic algae, zooplankton, and phytoplankton, which are major contributors to the origin of marine organic material.[40] Similarly, the lower values of the terrigenous/aquatic ratio (TAR) for the Patala (0.10), Lockhart (0.26), and Hangu (0.12) also indicate the marine source in these formations.[30,38,41] The carbon preference index (CPI) is determined after dividing the sum of the odd carbon number (C_{23}−C_{29}) by the sum of the even number (C_{22}−C_{30}) alkanes. The CPI values for these formations are 1.04, 0.91, and 0.95 respectively, which indicates that these rocks bear a high thermal maturity (Table 4). Acyclic isoprenoid compounds are present in the source rock extracts of the Paleocene units (Figure 14). The isoprenoid compounds include pristane (Pr) and phytane (Ph), which exist in all of these extracts derived from the Paleocene rocks.[36,37]

Lower ratio values between Pr and Ph (Pr/Ph < 3) were observed for the studied Patala, Lockhart, and Hangu formation samples. The Pr/Ph values for the Paleocene rock were 1.8, 1.23, and 1.33, respectively, which describe the type of organic matter

Table 6. Biomarker Parameters Derived from Terpanes by SIM-GC-MS Analysis[50]

parameters	Patala	Lockhart	Hangu
$C_{19}/C_{19} + C_{23}$ triterpanes	C_{23} present	C_{23} present	C_{23} present
	C_{19} is almost absent	C_{19} is almost absent	C_{19} is almost absent
C_{29}/H_{30} triterpanes	0.8	0.68	0.86
gammacerane/H_{30}	0.09	0.05	0.09
M_{30}/H_{30}	0.25	nil	0.04
Ts/Ts + Tm	0.50	0.49	0.50
$H_{32}S/H_{32}S + H_{32}R$	0.58	0.50	0.60
$C_{19}TCT/C_{19}TCT + C_{23}TCT$	0.14	0.14	0.08
$C_{24}TeCT/C_{24}TeCT + C_{23}TCT$	0.4	0.33	0.3
$C_{22}TCT/C_{21}TCT$	0.5	0.3	0.2
$C_{24}TCT/C_{23}TCT$	0.5	0.6	0.5
S/S + R HH_{32}	0.58	0.5	0.6

https://doi.org/10.1021/acsomega.3c09457
ACS Omega 2024, 9, 14123−14141

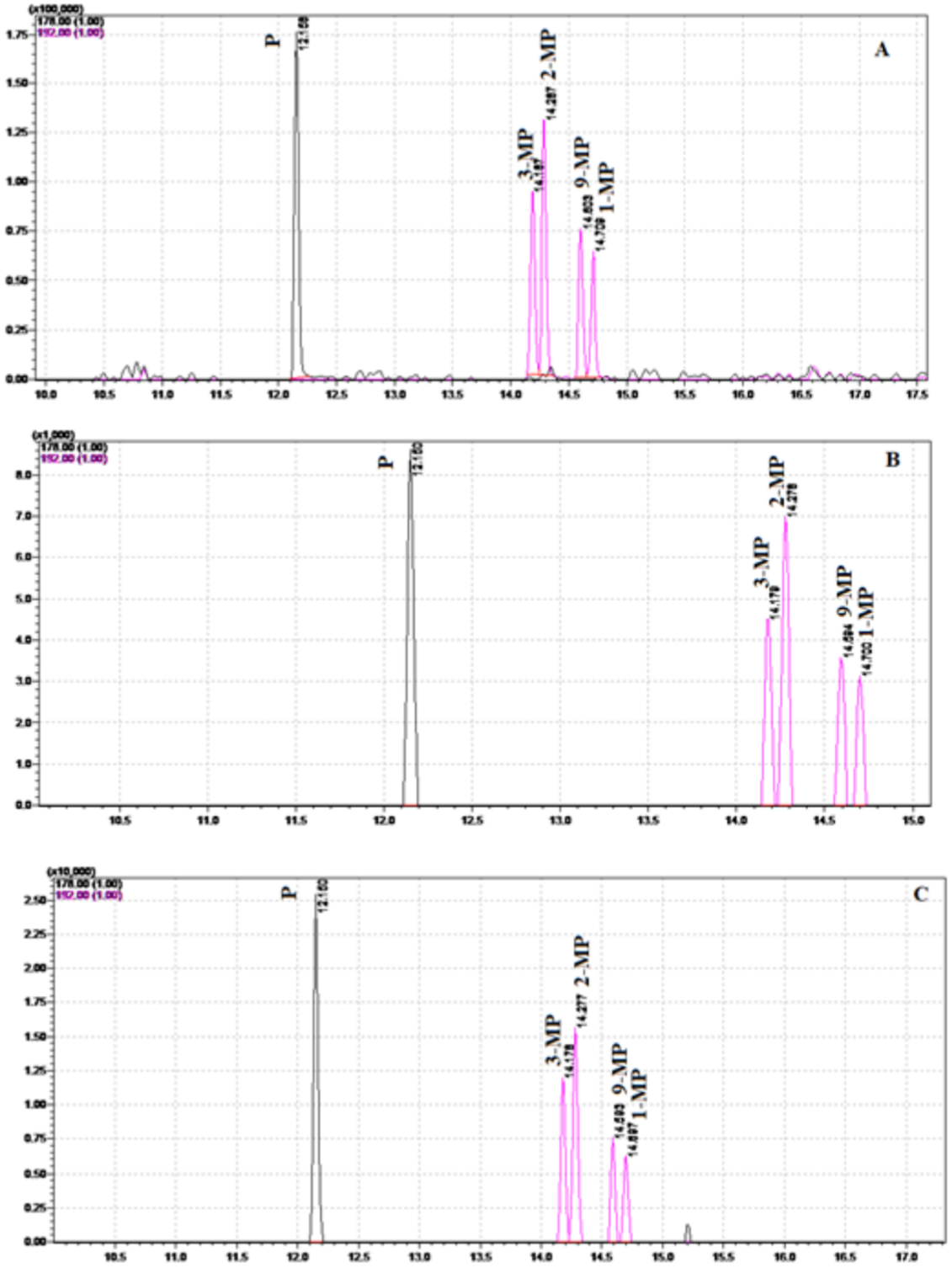

Figure 16. Combined mass chromatograms of m/z 178 + 192 showing phenanthrene (P) and methylphenanthrene (MP) in the aromatic fractions of (A) Patala, (B) Lockhart, and (C) Hangu.

present and depositional settings (Table 5).[42] These ratios, which are considered to be better indicators of depositional settings, reveal that the organic matter was deposited in a suboxic environment. The plot between Pr/n-C_{17} and Ph/n-C_{18} ratios indicates that the Paleocene units fall in the category of mixed organic matter source deposited in a transitional depositional setting (Figure 15). Very little or negligible effects of microbial activity (biodegradation) and variation of thermal maturity were observed (Figure 16).

4.3.2. Distribution of Terpanes and Steranes. Different ratios of tricyclic terpanes, tetracyclic terpanes, hopanes, moretanes, gammacerane, oleanane, and homohopanes can also be used to interpret the environment of deposition, source input, lithology of the source for oil, thermal maturity, age of organic matter, and oil−oil and oil-source correlation (Table 6).

https://doi.org/10.1021/acsomega.3c09457
ACS Omega 2024, 9, 14123−14141

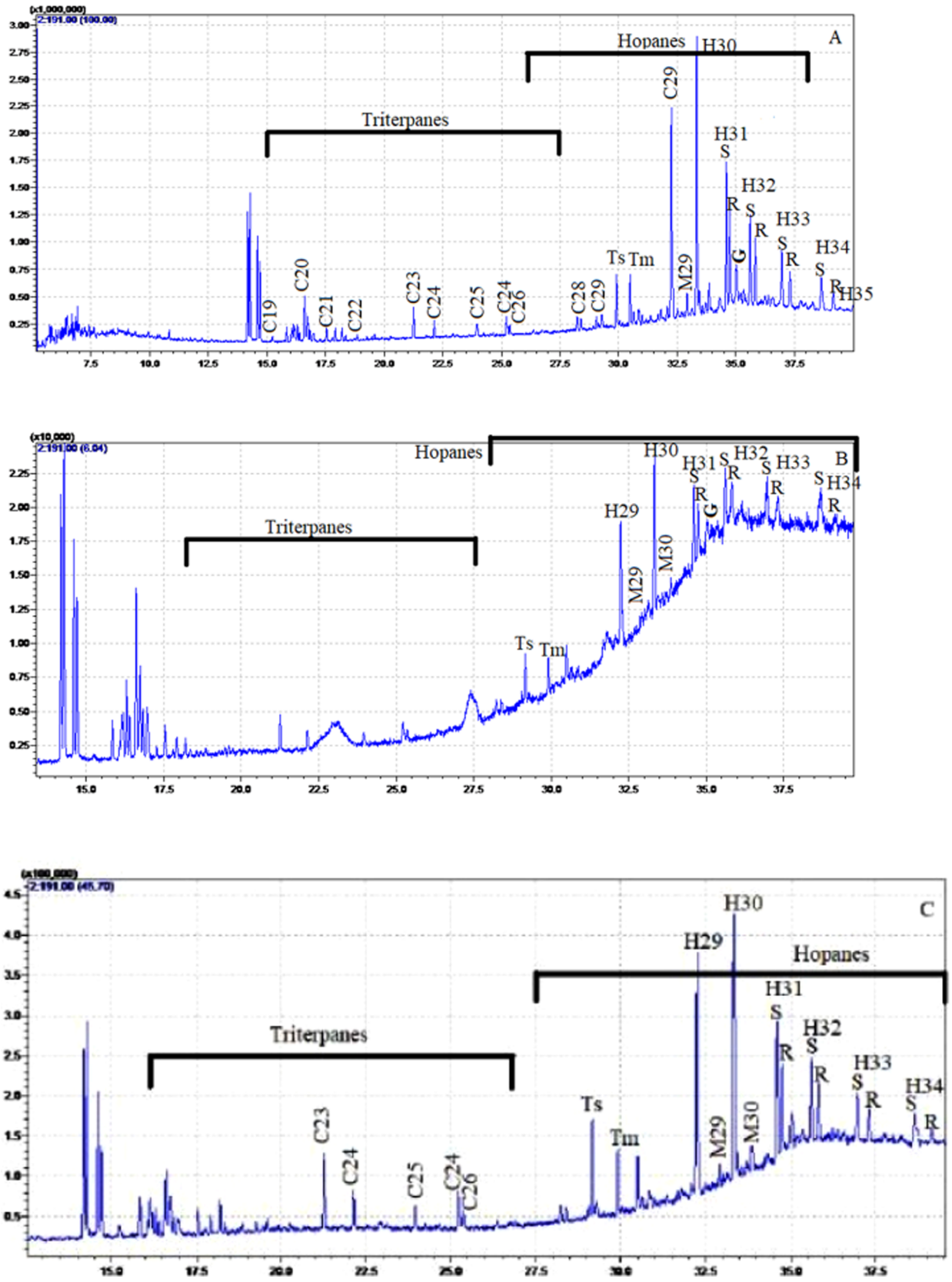

Figure 17. Mass chromatograms of m/z 191 showing terpanes and hopene extracts: (A) Patala formation, (B) Lockhart Limestone, and (C) Hangu formation.

The absence of C_{35} homohopanes in Hangu, Lockhart, and Patala's source rock extracts clearly indicates an oxic depositional environment (Figure 17). Gammacerane is a biomarker that is produced by protozoans living in freshwater and is formed by tetrahymanol, which is a precursor and is converted during diagenesis.[43] This biomarker was identified in

https://doi.org/10.1021/acsomega.3c09457
ACS Omega 2024, 9, 14123−14141

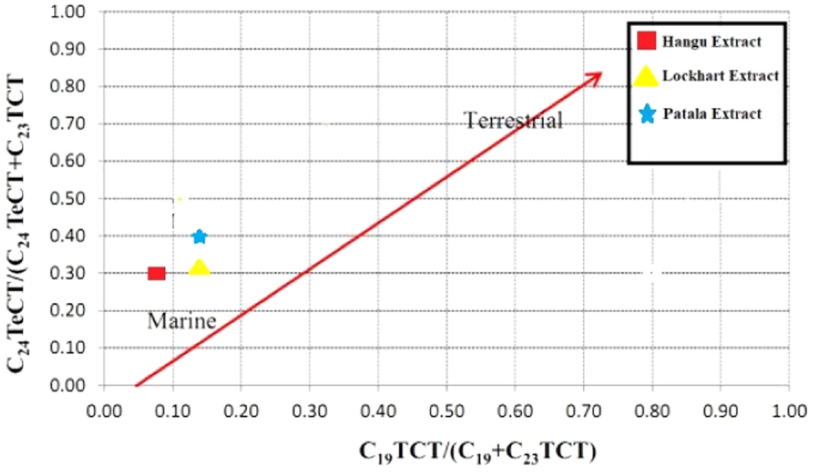

Figure 18. Cross-plot of $C_{19}TCT/(C_{19}TCT + C_{23}TCT)$ vs $C_{24}TeCT/(C_{24}TeCT + C_{23}TCT)$ (criteria adopted for classification from 45).

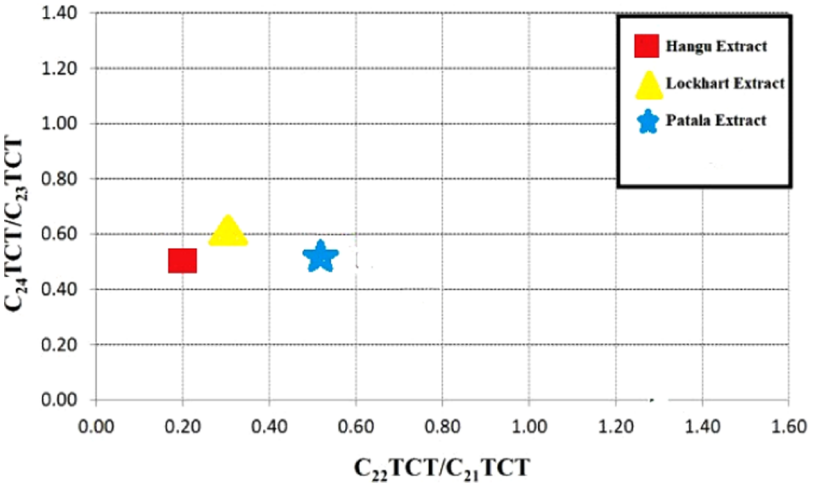

Figure 19. Cross-plot for $C_{24}TCT/C_{23}TCT$ vs $C_{22}TCT/C_{21}TCT$.

the rock extract samples of Paleocene units through the selective ion monitoring method using the fragmentogram of m/z 191 in GC-MS. The lower values of the gammacerance index (5−10%) indicate a very hypersaline marine deposition (Table 6).[44] The lower values of C_{19} TCT/C_{19} TCT + C_{23} TCT ratio, and the plot of $C_{19}TCT/C_{19}TCT + C_{23}TCT$ vs $C_{24}TeCT/C_{24}TeCT + C_{23}TCT$ also indicate that the extracts belong to the category of source derived from the marine input (Figure 18). Similarly, the lower values of the C_{29}/H_{30} ratio of the extracts from Patala (0.8), Lockhart (0.68), and Hangu (0.86) could be an indication of shale-derived oil. The lower values of $C_{22}TCT/C_{21}TCT$ compared to $C_{24}TCT/C_{23}TCT$ for Hangu and Lockhart formations indicate that the source input was clastic, while equal values of these ratios for the Patala formation show a carbonate source (Figure 19).[45−4647] Lower values of Moretane M_{30} to Hopane H_{30}, Ts ($C_{27}18\alpha$-22,29,30-trisnorneohopane)/Tm (17α-22,29,30-trisnorhopane), and S/S + R HH32 ratios indicate that the extracts of the Paleocene units belong to the thermally mature window (Table 6).[48,49]

Sterane distributions for the source rock extracts were studied through SIM/GC-MS using m/z 217 and 218 ions.[51] The ion chromatograms m/z 217 of the analyzed samples show distributions of C_{27}, C_{28}, and C_{29} regular steranes, and chromatograms m/z 218 show a relative abundance of $\beta\beta$ isomers of C_{27}, C_{28}, and C_{29} regular steranes (Figure 20). C_{27} steranes come from marine sources along with C_{28}, precursors usually abundant in phytoplankton and zooplankton, while C_{29} steranes are derived from terrestrial sources. Greater values (>1) of the C_{29}/C_{27} sterane ratios for Lockhart (2.04) and Hangu (1.72) show a higher land plant input, while the Patala formation (0.90) shows a higher marine input (Table 7). A ternary diagram of $C_{27}-C_{28}-C_{29}$ steranes shows a similar trend in which the origin of the organic matter present in the Patala formation is open marine.[52,53] In contrast, for both Hangu and Lockhart formations, organic matter was developed in terrestrial environments (Figure 21). A similar value of $C_{29}\beta\beta/C_{29}\beta\beta + C_{29}\alpha\alpha$ ratio was observed for the studied samples of Patala (0.51), Hangu (0.51), and Lockhart formations (0.49), which clearly indicates that the formations have not attained maturity of the late oil window.[54]

4.3.3. Distribution of Aromatic Compounds. Aromatic hydrocarbons can be effective for correlating oil with source rocks. Several indices and ratios can be used to calculate the thermal maturity stage of rock and oil with the help of biomarkers and aromatic hydrocarbons. Methylphenanthrene index (MPI) is a parameter used for thermal maturity prediction based on phenanthrene and four isomers of methylpehenanthrene.[55]

The presence of a higher quantity of more stable hopanes, i.e., 2MP and 3MP in all of the Paleocene rock extracts, shows

https://doi.org/10.1021/acsomega.3c09457
ACS Omega 2024, 9, 14123−14141

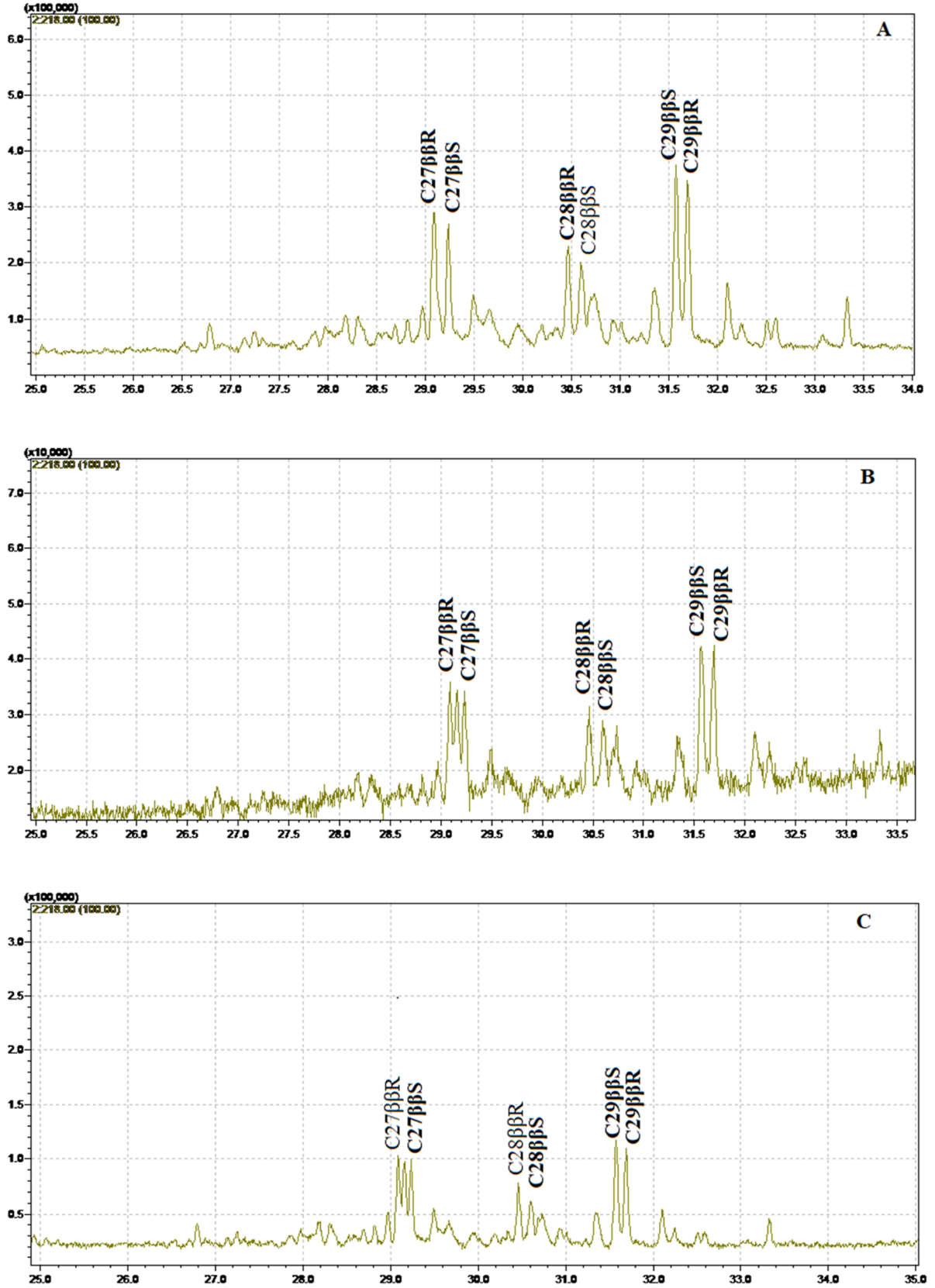

Figure 20. *m*/*z* 218 SIM chromatogram shows the distribution of C_{27}, C_{28}, and C_{29} steranes for (A) Patala, (B) Lockhart, and (C) Hangu.

relatively higher thermal maturity, as shown in Figure 22. Both MPI-3 and MPR-1 values for Hangu and Lockhart extracts show medium to high thermal maturity, as shown in Table 8.

5. DISCUSSION

In the current study, geochemical and biomarker parameters were determined to evaluate the nature of the organic matter,

https://doi.org/10.1021/acsomega.3c09457
ACS Omega 2024, 9, 14123−14141

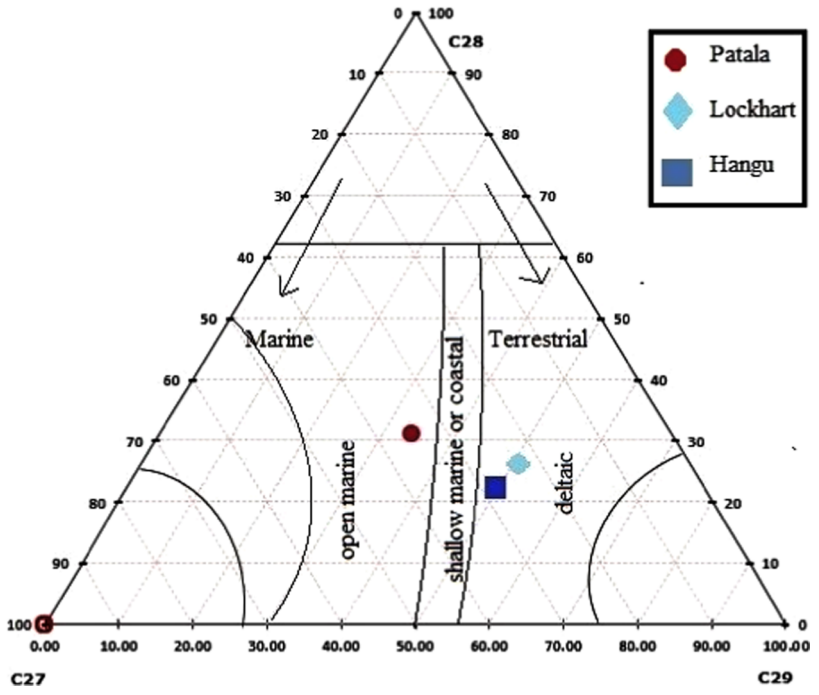

Figure 21. Ternary diagram showing the distribution of regular steranes C_{27}, C_{28}, and C_{29} for Patala, Lockhart, and Hangu.

depositional settings, and thermal maturity of the Patala, Lockhart, and Hangu formations in the Kohat sub-basin. In the Kohat sub-basin, the source rock potential has not been very well studied, particularly for Paleocene formations. Several studies have been conducted to evaluate the source rock potential of the Paleocene Patala formation, which acts as a primary source rock in the Potwar basin lying in the east of the study area.[13,21] Other Paleocene units, including Lockhart and Hangu, bear a strong source rock potential, which was also reported in other studies in the Potwar basin.[56−575859] Generally, the TOC values in the Patala formation lie between 0.5% and greater than 3.5% in the Potwar Plateau, Upper Indus Basin of Pakistan.[21] The Lockhart formation also bears a good source rock potential in the basin, with an average value of TOC $\geq$ 1.4%.[59] In the study area, lower TOC (<0.5%) values were observed for the Patala formation, indicating its weaker potential to generate hydrocarbons. In this study, efforts were made to assess the potential of these Paleocene units using drill cuttings obtained from the HDIP. The lower TOC values are attributed to the study area's tectonic pattern, geological position, and structural trends.[60] The TOC values at present do not reflect the original or total organic matter because over time and with the increase in thermal maturity, kerogen is converted into hydrocarbons and the value of TOC decreases. A lower TOC (<0.5%) may produce and be a possible source rock and act as a secondary source rock.[61]

Hangu formation having HI value less than 200 mostly falls in the category of Type III. Lockhart Limestone and Patala formation having HI values in the range of less than 100−250 fall in the category of Type-III kerogen. The Patala formation in the Potwar basin mostly belongs to Types II and III and is thermally mature.[21] In the study area, the Patala unit showed lower thermal maturity. OEP can also be used to predict thermal maturity parameters; therefore, with an increase in thermal maturity, this effect will disappear.[38] The presence of this type of distribution in the Hangu formation and Lockhart Limestone is in the thermally mature zone, with values of approximately 1. On the contrary, Lockhart and Hangu formations are thermally mature. Several factors, including burial depth, level of tectonic deformation, and structural pattern, control the thermal maturity in the study area. The thermal maturity of the Paleocene units corresponds to subsurface temperatures in the range 90−150 °C (oil window). Due to financial constraints, biomarker studies were also conducted with fewer samples taken from HDIP. Biomarker analysis on the rock extracts of Paleocene units provided a general idea of the units as potential source rock. An in-depth study with more rock and outcrop samples is required to further assess the source potential of the Paleocene units in the sub-basin.

6. CONCLUSIONS

Detailed geochemical studies were conducted on drill cuttings and rock extracts of the Paleocene rocks in the Kohat sub-basin to estimate the source-rock potential of the Paleocene units using total organic carbon (TOC), Rock-Eval pyrolysis, organic petrography (vitrinite reflectance), column chromatography, and gas chromatography−mass spectrometry (GC−MS).

- The Hangu formation shows poor to good TOC content (wt %), while both the Lockhart and Patala formations belong to the poor to fair TOC content (wt %) category. Rock-Eval pyrolysis indicates that the source potential of the Lockhart and Hangu formations is in the mature stage of oil and gas production.
- The Pr/Ph ratios for the Hangu (1.33), Lockhart Limestone (1.23), and Patala formation (1.80) show that the organic content was formed in a suboxic depositional environment (1 > Pr/Ph < 3). The vitrinite reflectance values are in the range of 0.82−0.95%.
- The lower ratios between $C_{19}TCT/(C_{19}TCT + C_{23}TCT)$, $C_{24}TeCT/(C_{24}TeCT + C_{23}TCT)$, and $C_{24}TeCT/C_{24}TeCT + C_{23}TCT$ represent marine depositional environments. Additionally, the source input (lithology) was defined using the C_{29}/H_{30} ratio,

https://doi.org/10.1021/acsomega.3c09457
ACS Omega 2024, 9, 14123−14141

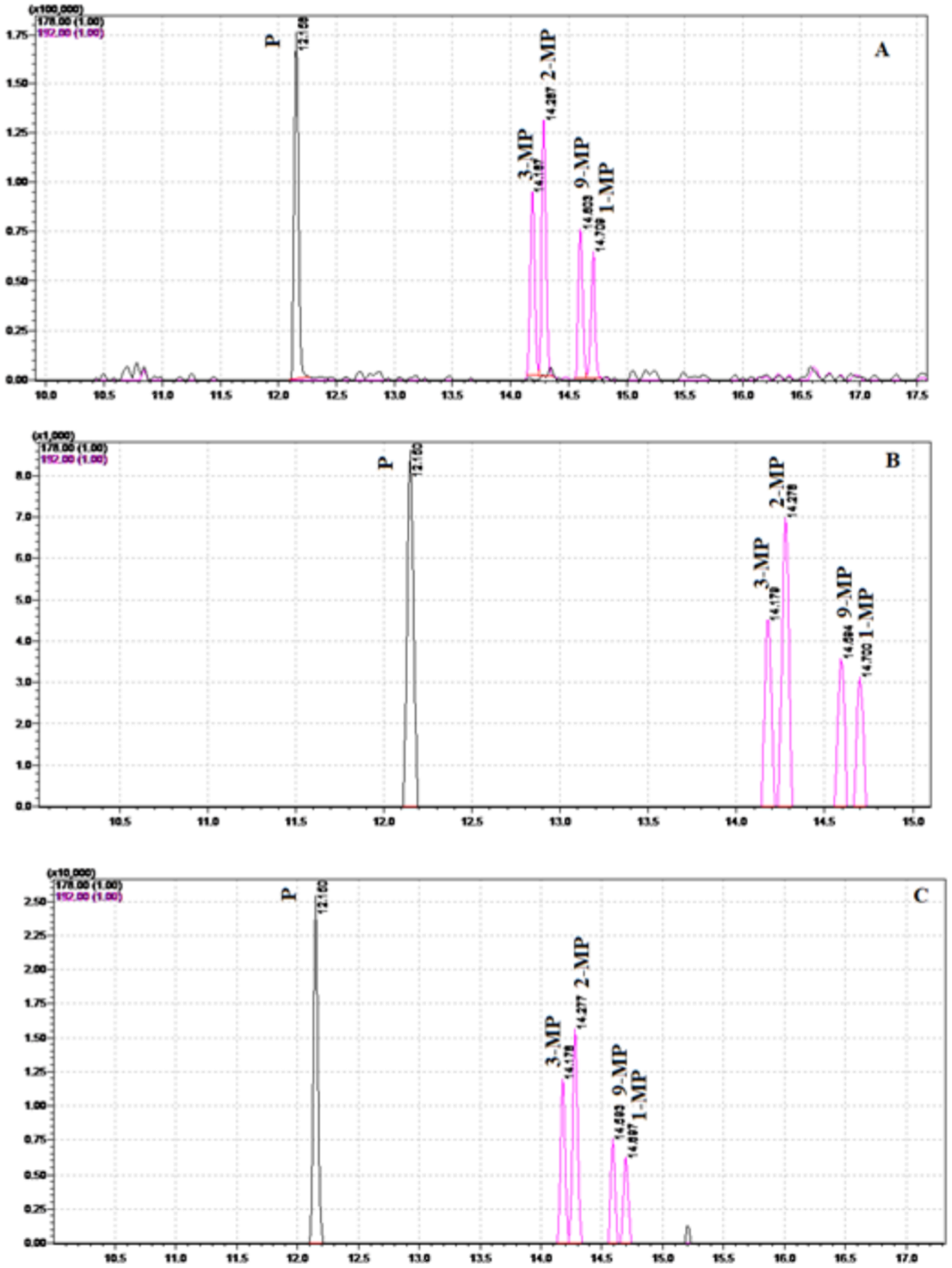

Figure 22. Combined mass chromatograms of *m*/*z* 178 + 192 showing phenanthrene (P) and methylphenanthrene (MP) in aromatic fractions of (A) Patala, (B) Lockhart, and (C) Hangu.

which indicates that Hangu (0.86), Lockhart (0.68), and Patala (0.80) comprised shale lithology.

- The ternary diagram of regular steranes indicates a higher plant input in the Hangu and Lockhart samples, falling in the terrestrial source region. On the other hand, the Patala formation bears a comparatively higher marine input.
- The thermal maturity of the sediment extracts shows a higher thermal maturity and mature oil zone. In general, the GP value lies in a poor class, except for a few samples extracted from the Hangu and Lockhart formations, which correspond to a fair potential class. Lower CPI values for Hangu (0.95), Lockhart (0.91), and Patala (1.04) indicate a higher thermal maturity.
- The presence of more stable isotopes such as 2MP and 3MP in extracts from Hangu and Lockhart shows relatively higher thermal maturity. The M_{30} to C_{30}

https://doi.org/10.1021/acsomega.3c09457
ACS Omega 2024, 9, 14123−14141

Hopane values for this ratio for Hangu (0.04) and Patala (0.25) fall in the thermally mature window. The value of the (Ts/Ts + Tm) ratio from the extracts also shows the same results for thermal maturity. Sterane [C29$\beta\beta$/(C29$\beta\beta$ + C29$\alpha\alpha$)] values show that the present status of the Hangu, Lockhart, and Patala formations are mature and fall in the oil window.

AUTHOR INFORMATION

Corresponding Authors

Muhsan Ehsan − *Department of Earth and Environmental Sciences, Bahria School of Engineering and Applied Sciences, Bahria University, Islamabad 44000, Pakistan*; orcid.org/0000-0001-9430-5486; Email: muhsanehsan98@hotmail.com

Abid Ali − *Institute of Geology, University of the Punjab, Lahore 54000, Pakistan*; Email: abidali306@gmail.com

Authors

Jazeb Sohail − *Department of Earth and Environmental Sciences, Bahria School of Engineering and Applied Sciences, Bahria University, Islamabad 44000, Pakistan*

Saqib Mehmood − *Department of Earth and Environmental Sciences, Bahria School of Engineering and Applied Sciences, Bahria University, Islamabad 44000, Pakistan*

Samina Jahandad − *Hydrocarbon Development Institute of Pakistan (HDIP), Islamabad 44000, Pakistan*

Kamal Abdelrahman − *Department of Geology and Geophysics, College of Science, King Saud University, Riyadh 11451, Saudi Arabia*

S. M. Talha Qadri − *School of Land Use and Environmental Change, University of the Fraser Valley, Abbotsford, British Columbia V2S 7M8, Canada*

Mohammed S. Fnais − *Department of Geology and Geophysics, College of Science, King Saud University, Riyadh 11451, Saudi Arabia*

Complete contact information is available at: https://pubs.acs.org/10.1021/acsomega.3c09457

Author Contributions

#J.S. and M.E. contributed equally to this work. First authorship is shared between J.S. and M.E.

Notes

The authors declare no competing financial interest.

ACKNOWLEDGMENTS

WE would like to thank the Researchers Supporting Project number (RSP2024R351), King Saud University, Riyadh, Saudi Arabia, for funding this research. The authors would like to express their utmost gratitude to the Directorate General of Petroleum Concession (DGPC) of Pakistan for providing the essential data required for this research. Furthermore, our special thanks and appreciation to the Hydrocarbon Development Institute of Pakistan (HDIP) for providing lab facilities to perform this research work. The work is also submitted to the Higher Education Commission (HEC), Pakistan repository, to award the MS degree to J.S.

REFERENCES

(1) Li, J.; Wang, Y.; Nguyen, X.; Zhuang, X.; Li, J.; Querol, X.; Li, B.; Moreno, N.; Hoang, V.; Cordoba, P.; Do, V. First insights into mineralogy, geochemistry, and isotopic signatures of the Upper Triassic high-sulfur coals from the Thai Nguyen Coal field, NE Vietnam. *Int. J. Coal Geol.* **2022**, *261*, No. 104097.

(2) Xu, Z.; Li, X.; Li, J.; Xue, Y.; Jiang, S.; Liu, L.; Luo, Q.; Wu, K.; Zhang, N.; Feng, Y.; Shao, M.; Jia, K.; Sun, Q. Characteristics of Source Rocks and Genetic Origins of Natural Gas in Deep Formations, Gudian Depression, Songliao Basin, NE China. *ACS Earth Space Chem.* **2022**, *6* (7), 1750−1771.

(3) Ren, C.; Yu, J.; Liu, S.; Yao, W.; Zhu, Y.; Liu, X. A Plastic Strain-Induced Damage Model of Porous Rock Suitable for Different Stress Paths. *Rock Mech. Rock Eng.* **2022**, *55* (4), 1887−1906.

(4) Xiao, D.; Liu, M.; Li, L.; Cai, X.; Qin, S.; Gao, R.; Liu, J.; Liu, X.; Tang, H.; Li, G. Model for economic evaluation of closed-loop geothermal systems based on net present value. *Appl. Therm. Eng.* **2023**, *231*, No. 121008.

(5) Xu, K.; Yang, H.; Zhang, H.; Ju, W.; Li, C.; Fang, L.; Wang, Z.; Wang, H.; Yuan, F.; Zhao, B.; et al. Fracture effectiveness evaluation in ultra-deep reservoirs based on geomechanical method, Kuqa Depression, Tarim Basin, NW China. *J. Pet. Sci. Eng.* **2022**, *215*, No. 110604.

(6) Kabeyi, M. J. B.; Olanrewaju, O. A. Sustainable Energy Transition for Renewable and Low Carbon Grid Electricity Generation and Supply. *Front. Energy Res.* **2022**, *9*, 743114.

(7) BP. *Energy Outlook*, 2020; p 158.

(8) Tie, Y.; Rui, X.; Shi-Hui, S.; Zhao-Kai, H.; Jin-Yu, F. A real-time intelligent lithology identification method based on a dynamic felling strategy weighted random forest algorithm. *Pet. Sci.* **2023**, DOI: 10.1016/j.petsci.2023.09.011.

(9) Yang, L.; Wang, H.; Xu, H.; Guo, D.; Li, M. Experimental study on characteristics of water imbibition and ion diffusion in shale reservoirs. *Geoenergy Sci. Eng.* **2023**, *229*, No. 212167.

(10) Wu, M.; Ba, Z.; Liang, J. A procedure for 3D simulation of seismic wave propagation considering source-path-site effects: Theory, verification and application. *Earthquake Eng. Struct. Dyn.* **2022**, *51* (12), 2925−2955.

(11) Khan, H. K.; Ehsan, M.; Ali, A.; Amer, M. A.; Aziz, H.; Khan, A.; Bashir, Y.; Abu-Alam, T.; Abioui, M. Source rock geochemical assessment and estimation of TOC using well logs and geochemical data of Talhar Shale, Southern Indus Basin, Pakistan. *Front. Earth Sci.* **2022**, *10*, No. 969936.

(12) Wang, Y.; Lou, M.; Wang, Y.; Fan, C.; Tian, C.; Qi, X. Experimental investigation of the effect of rotation rate and current speed on the dynamic response of riserless rotating drill string. *Ocean Eng.* **2023**, *280*, No. 114542.

(13) Yasin, Q.; Baklouti, S.; Khalid, P.; Ali, S. H.; Boateng, C. D.; Du, Q. Evaluation of shale gas reservoirs in complex structural enclosures: A case study from Patala Formation in the Kohat-Potwar Plateau, Pakistan. *J. Pet. Sci. Eng.* **2021**, *198*, No. 108225.

(14) Yasin, Q.; Baklouti, S.; Sohail, G. M.; Asif, M.; Xufei, G. Evaluation of Neoproterozoic source rock potential in SE Pakistan and adjacent Bikaner−Nagaur Basin India. *Sci. Rep.* **2022**, *12* (1), No. 11102.

(15) Yao, W.; Yu, J.; Liu, X.; Zhang, Z.; Feng, X.; Cai, Y. Experimental and theoretical investigation of coupled damage of rock under combined disturbance. *Int. J. Rock Mech. Min. Sci.* **2023**, *164*, No. 105355.

(16) Rui, S.; Zhou, Z.; Jostad, H. P.; Wang, L.; Guo, Z. Numerical prediction of potential 3-dimensional seabed trench profiles considering complex motions of mooring line. *Appl. Ocean Res.* **2023**, *139*, No. 103704.

(17) Riaz, M.; Nuno, P.; Zafar, T.; Ghazi, S. 2D Seismic Interpretation of the Meyal Area, Northern Potwar Deform Zone, Potwar Basin, Pakistan. *J. Open Geosci.* **2019**, *11*, No. e01, DOI: 10.1515/geo-2019-0001.

(18) Fazeelat, T.; Jalees, M.; Bianchi, T. Source rock potential of Eocene, Paleocene and Jurassic deposits in the subsurface of the Potwar Basin, northern Pakistan. *J. Pet. Geol.* **2010**, *33* (1), 87−96.

(19) Ehsan, M.; Latif, M. A. U.; Ali, A.; Radwan, A. E.; Amer, M. A.; Abdelrahman, K. Geocellular Modeling of the Cambrian to Eocene

Multi-Reservoirs, Upper Indus Basin, Pakistan. *Nat. Resour. Res.* **2023**, *32* (6), 2583−2607.
(20) Sohail, G. M.; Hawkes, C. D.; Yasin, Q. An integrated petrophysical and geomechanical characterization of Sembar Shale in the Lower Indus Basin, Pakistan, using well logs and seismic data. *J. Nat. Gas Sci. Eng.* **2020**, *78*, No. 103327.
(21) Wandrey, C. J.; Law, B.; Shah, H. A. *Patala-Nammal Composite Total Petroleum System, Kohat-Potwar Geologic Province, Pakistan* US Department of the Interior, US Geological Survey: 2004.
(22) Amjad, M. R.; Ehsan, M.; Hussain, M.; Al-Ansari, N.; Rehman, A.; Naseer, Z.; Ejaz, M. N.; Baouche, R.; Elbeltagi, A. Carbonate Reservoir Quality Variations in Basins with a Variable Sediment Influx: A Case Study from the Balkassar Oil Field, Potwar, Pakistan. *ACS Omega* **2023**, *8* (4), 4127−4145.
(23) Searle, M. P.; Kahn, M. A. Geological Map of North Pakistan and Adjacent Areas of Northern Ladakh and Western Tibet.(Western Himalaya, Salt Ranges, Kohistan, Karakoram, Hindu Kush), 1:650 000, 1996.
(24) Malkani, M. S.; Mahmood, Z. Stratigraphy of Pakistan. Geological Survey of Pakistan. *Memoir* **2017**, *24*, 1−134.
(25) Barker, C. Petroleum geochemistry in exploration and development: Part 1—Principles and processes. *Leading Edge* **1999**, *18* (6), 678−684.
(26) Bjorlykke, K. *Petroleum Geoscience: From Sedimentary Environments to Rock Physics*; Springer Science & Business Media, 2010.
(27) Golin, V.; Smyth, M. Depositional environments and hydrocarbon potential of the Evergreen Formation, ATP 145P, Surat Basin, Queensland. *APPEA J.* **1986**, *26* (1), 156−171.
(28) Peters, K. E.; Cassa, M. R. *Applied Source Rock Geochemistry*; Memoirs − American Association of Petroleum Geologists, 1994; p 93.
(29) Cooles, G. P.; Mackenzie, A. S.; Quigley, T. M. Calculation of petroleum masses generated and expelled from source rocks. *Org. Geochem.* **1986**, *10* (1), 235−245.
(30) Tissot, B. P.; Welte, D. H. *Petroleum Formation and Occurrence*; Springer-Verlag: Heidelberg, 1984; p 699.
(31) Hunt, J. *Petroleum Geochemistry and Geology*, 2nd ed.; W. H. Freeman, 1996.
(32) Pitman, J. K.; Franczyk, K. J.; Anders, D. E. Marine and nonmarine gas-bearing rocks in Upper Cretaceous Blackhawk and Neslen formations, eastern Uinta Basin, Utah: sedimentology, diagenesis, and source rock potential. *AAPG Bull.* **1987**, *71* (1), 76−94, DOI: 10.1306/94886D4E-1704-11D7-8645000102C1865D.
(33) Tissot, B.; Demaison, G.; Masson, P.; Delteil, J. R.; Combaz, A. Paleoenvironment and petroleum potential of middle Cretaceous black shales in Atlantic basins. *AAPG Bull.* **1980**, *64* (12), 2051−2063, DOI: 10.1306/2F919738-16CE-11D7-8645000102C1865D.
(34) Smyth, M.; Mastalerz, M. Organic petrological composition of Triassic source rocks and their clastic depositional environments in some Australian sedimentary basins. *Int. J. Coal Geol.* **1991**, *18* (3−4), 165−186.
(35) Welte, D. H.; Horsfield, H.; Baker, D. R. *Petroleum and Basin Evolution*; Springer-Verlag: New York, 1997; pp 1−525.
(36) Peters, K. E.; Moldowan, J. M. *The Biomarker Guide: Interpreting Molecular Fossils in Petroleum and Ancient Sediments*; Prentice Hall: United States, 1993; p 363.
(37) Waples, D. W. *Geochemistry in Petroleum Exploration*; D. Reidel Publishing Company: Dordrecht, Holland, 1985; p 232.
(38) Peters, K. E.; Walters, C. C.; Moldowan, J. M. *The Biomarker Guide: Biomarkers and Isotopes in the Environment and Human History*; Cambridge University Press, 2005; Vol. *1*.
(39) Nishimura, M.; Baker, E. W. Possible origin of n-alkanes with a remarkable even-to-odd predominance in recent marine sediments. *Geochim. Cosmochim. Acta* **1986**, *50* (2), 299−305.
(40) Wang, Y.; Yang, H.; Zhang, J.; Gao, W.; Huang, C.; Xie, B. Characterization of n-alkanes and their carbon isotopic composition in sediments from a small catchment of the Dianchi watershed. *Chemosphere* **2015**, *119*, 1346−1352.
(41) Jones, P. J.; Philp, R. P. Oils and source rocks from Pauls Valley, Anadarko basin, Oklahoma, USA. *Appl. Geochem.* **1990**, *5* (4), 429−448.
(42) Didyk, B. M.; Simoneit, B. R. T.; Brassell, S. C. t.; Eglinton, G. Organic geochemical indicators of palaeoenvironmental conditions of sedimentation. *Nature* **1978**, *272* (5650), 216−222.
(43) Rangel, A.; Parra, P.; Niño, C. The La Luna formation: chemostratigraphy and organic facies in the Middle Magdalena Basin. *Org. Geochem.* **2000**, *31* (12), 1267−1284.
(44) Damsté, J. S. S.; Kenig, F.; Koopmans, M. P.; Köster, J.; Schouten, S.; Hayes, J. M.; de Leeuw, J. W. Evidence for gammacerane as an indicator of water column stratification. *Geochim. Cosmochim. Acta* **1995**, *59* (9), 1895−1900.
(45) Zumberge, J. E.Tricyclic Diterpane Distributions in the Correlation of Paleozoic Crude Oils from the Williston Basin. In *Advances in Organic Geochemistry*; Wiley, 1981; pp 738−745.
(46) Tan, Z.; Guo, J.; Huang, H. Chemometric Classification of Oil Families in the Laizhouwan Depression, Bohai Bay Basin, Eastern China. *ACS Omega* **2021**, *6* (37), 24106−24117.
(47) Connan, J.; Dessort, D. Novel family of hexacyclic hopanoid alkanes (C32— C35) occurring in sediments and oils from anoxic paleoenvironments. *Org. Geochem.* **1987**, *11* (2), 103−113.
(48) Tessin, A.; Bianchi, T. S.; Sheldon, N. D.; Hendy, I.; Hutchings, J. A.; Arnold, T. E. Organic matter source and thermal maturity within the Late Cretaceous Niobrara Formation, US Western Interior. *Mar. Pet. Geol.* **2017**, *86*, 812−822.
(49) Kara-Gülbay, R.; Korkmaz, S. Element Contents and Organic Matter− Element Relationship of the Tertiary Oil Shale Deposits in Northwest Anatolia, Turkey. *Energy Fuels* **2008**, *22* (5), 3164−3173.
(50) Ma, X.; Wei, L.; Hou, D.; Xu, C.; Man, Y.; Li, W.; Wu, P. Geochemical Characteristics of Three Oil Families and Their Possible Source Rocks in the Sub-Sag A of Weixinan Depression, Beibuwan Basin, Offshore South China Sea. *ACS Omega* **2022**, *7* (28), 24795−24811.
(51) Liu, S.; Gao, G.; Jin, J.; Gang, W.; Xiang, B. Source rock with high abundance of C28 regular sterane in typical brackish-saline lacustrine sediments: Biogenic source, depositional environment and hydrocarbon generation potential in Junggar Basin, China. *J. Pet. Sci. Eng.* **2022**, *208*, No. 109670.
(52) Hammad, M. M.; El Nady, M. M. Oil−Source Rocks Correlation Based on the Biomarker Distribution of EWD and Qarun Oilfields, North Western Desert, Egypt. *Pet. Sci. Technol.* **2012**, *30* (2), 133−146.
(53) Sampei, Y.; Matsumoto, E. C/N ratios in a sediment core from Nakaumi Lagoon, southwest Japan—usefulness as an organic source indicator—. *Geochem. J.* **2001**, *35* (3), 189−205.
(54) Seifert, W. K.; Moldowan, J. M.; Demaison, G. J. Source correlation of biodegraded oils. *Org. Geochem.* **1984**, *6*, 633−643.
(55) Welte, D. H.; Yükler, M. A.; Radke, M.; Leythaeuser, D.; Mann, U.; Ritter, U. *Organic Geochemistry and Basin Modelling − Important Tools in Petroleum Exploration*; Geological Society: London, 1983; Vol. *12*, pp 237−252.
(56) Jalees, M. I.; Tahira, F. Geochemical segregation of early Permian, Paleocene and Eocene sediments of Potwar Basin, Pakistan: I Geophysical and isotopic analysis for source and depositional environment. *Carbonates Evaporites* **2020**, *35* (2), 63.
(57) Quadri, V.; Quadri, S. M. G. J. Exploration anatomy of success in oil and gas exploration in Pakistan. *Oil Gas J.* **1996**, *94* (20), No. e1.
(58) Latif, M. A. U.; Ehsan, M.; Ali, M.; Ali, A.; Ekoa Bessa, A. Z.; Abioui, M. The assessment of reservoir potential of Permian to Eocene reservoirs of Minwal-Joyamair fields, upper Indus basin, Pakistan. *Heliyon* **2023**, *9* (6), No. e16517.
(59) Jaswal, T. M.; Lillie, R. J.; Lawrence, R. D. Structure and evolution of the northern Potwar deformed zone. *AAPG Bull.* **1997**, *81*, 308−328, DOI: 10.1306/522B431B-1727-11D7-8645000102C1865D.
(60) Paracha, W. Kohat plateau with reference to Himalayan tectonic general study. *CSEG Rec.* **2004**, *29* (4), 126−134.
(61) Pang, B.; Chen, J.; Pang, X.; Liu, T.; Yang, H.; Li, H.; Wang, Y.; Hu, T. Possible new method to discriminate effective source rocks in

petroliferous basins: A case study in the Tazhong area, Tarim Basin.
Energy Explor. Exploit. **2020**, *38* (2), 417−433.

https://doi.org/10.1021/acsomega.3c09457
ACS Omega 2024, 9, 14123−14141